Received ; | Revised ; | Accepted

DOI: xxx/xxxx

RESEARCH ARTICLE

An improved nonlinear anisotropic PDE with $p(x)$-growth conditions applied to image restoration and enhancement

Hamza Alaa | Nour Eddine Alaa | Anass Bouchriti | Abderrahim Charkaoui*

[1]Laboratory LAMAI, Cadi Ayyad University, Faculty of Science and Technology, Marrakesh, Morocco

Correspondence
*Corresponding A. Charkaoui, Email: abderrahim.charkaoui@edu.uca.ma

Summary

This work proposes a novel nonlinear parabolic equation with $p(x)$-growth conditions for image restoration and enhancement. Based on the generalized Lebesgue and Sobolev spaces with variable exponent, we demonstrate the well-posedness of the proposed model. As a first result, we prove the existence of a weak solution to our model when the reaction term is bounded by a suitable function. Secondly, we use the approximations method to establish the existence of a nonnegative weak SOLA solution (Solution Obtained as Limit of Approximations) to the proposed model. Finally, numerical experiments illustrate that the proposed model performs better for image enhancement and denoising.

KEYWORDS:
Image enhancement and denoising, Nonlinear PDE, $p(x)$-growth, Schauder fixed point, Variable exponent, Weak solution

1 | STATEMENT OF THE PROBLEM

Digital image analysis gradually attracts more attention for its manifold of application. Along with academics, scientific, industrial and military use, a noticeable trend speaks of Metaverse [39]: A simulated digital environment above the physical to design settings that allow for rich user interaction in a way that resembles the real world. What we define in the real world as a material object, is referred to by Non-Fungible Token (NFT) in Metaverse. Images are considered one of the main NFTs and their analysis is crucial.

Image enhancement marks a preprocessing stage in digital image analysis. It highlights or sharpens image elements such as edges, boundaries, or contrast to make a visual display more useful for presentation and analysis. Unlike what is often thought, the enhancement does not increase the data's inherent information richness, but it does extend the dynamic range of the selected features, making them easier to identify. The most difficult aspect of image enhancement is quantifying the enhancement criterion; as a result, many image enhancement approaches are empirical and need participatory procedures to achieve desirable results. Among thee, are spatial and frequency domain techniques.

The latter enhance an image by convolving it with a generally linear position invariant operator. Such as for instance, The 2D convolution is carried out in the frequency domain using the Discrete Fourier Transform [9]. It is often used in Linear filtering [18], root filtering [29], Homomorphic filtering and pseudocoloring [23].

On the other hand, spatial domain enhancement techniques, which are based on direct manipulation of pixels in an image, are implemented to the image plane itself. They are further divided into two categories: Spatial filtering methods such as contour detection [21], noise smoothing [45], zooming [57], median filtering [59], etc. Overall, they are very powerful linear methods. Then there is point processing techniques which are based only on the intensity of single pixels. Such includes contrast stretching [34], noise clipping [27], histogram modeling [43], etc. They often rely on nonlinear operators but are generally simple to implement.

Among the latter tools relies our subject of interest: the application of partial differential equations (PDEs). It is a deeply anchored area in digital image processing that initiated in 1984 by investigating the famous parabolic heat equation. If we are to let Ω be an open bounded subset of $\mathbb{R}^N$ with a smooth boundary $\partial\Omega$. An image u, is then restored from a noisy image $u_0 = u + noise$ by the class of isotropic diffusion filter

$$\begin{cases} \partial_t u - \Delta u = 0 & \text{in } Q_T \\ u(0,x) = u_0(x) & \text{in } \Omega \\ \dfrac{\partial u}{\partial \nu} = 0 & \text{on } \Sigma_T, \end{cases}$$

where for a $T > 0$, $Q_T := (0,T)\times\Omega$, $\Sigma_T := (0,T)\times\partial\Omega$ and ν denotes the outward unit normal to $\partial\Omega$. Starting with changes at low intensities corresponding to image noise, the heat equation reduces all variations of the image. A somehow similar effect to the Gaussian smoothing as originally stated by Koenderink (1984) in [35]. However, a serious drawback of the method manifested in blurring and distorting the image as the smoothing effect do not differentiate noise from edges and contours which must be preserved. This is mainly due to the linearity of Laplacian Δ. While linear image enhancement methods are typically acceptable in many situations, nonlinear image enhancement approaches can give considerable benefits. This is owing largely to the fact that they effectively preserve image edges and details, whereas methods based on linear operators, such as the Laplacian, have a tendency to distort and blur them. According to Fan et al's research[25], nonlinear image enhancing methods are also less vulnerable to noise.

Because of the physical randomness of image acquisition systems, noise is always present. For example, physical constraints and sensor illumination levels lead to images with granularity noise which, together with transmission line defects, are captured during the digitization process.

To achieve the objectives that have been put forth previously, an attempt was proposed in 1990 by Perona-Malik[50]. It reads the subsequent equation

$$\begin{cases} \partial_t u - \operatorname{div}\left(g(|\nabla u|,\lambda)\nabla u\right) = 0 & \text{in } Q_T \\ u(0,x) = u_0(x) & \text{in } \Omega \\ \dfrac{\partial u}{\partial \nu} = 0 & \text{on } \Sigma_T, \end{cases}$$

where g is a nonnegative decreasing function that depends on the gradient norm such that $\lim\limits_{s\to\infty} g(s,\lambda) = 0$ and $g(0,\lambda) = 1$. The functional g is commonly refereed to as the diffusion coefficient.

The problem with the linear approach being the difficulty to obtain accurately the locations of the semantically meaningful edges at coarse scales was shown to be plainly related to the constant diffusion coefficient. Such is the case for the above Heat equation.

Driven by the unnecessity for such coefficient to be constant, Perona and Malik investigations lead to the development of the above equation. A nonlinear anistropic diffusion operator was shown to solve the blurring and localisation problems of linear diffusion filtering. They proposed multiple choices for the diffusion coefficient among which are

$$g(|\nabla u|,\lambda) = \frac{d}{1+\left(\frac{|\nabla u|}{\lambda}\right)^2} \quad \text{or} \quad g(|\nabla u|,\lambda) = d\,\exp\left(-\left(\frac{|\nabla u|}{\lambda}\right)^2\right),$$

where the coefficient d is a nonnegative constant and λ is a parameter that can be tweaked to preserve the image's edges.

The diffusion coefficient is set to vary spatially to favor intraregional smoothing over interregional smoothing; A somehow adaptive technique to separate noise from edges and contours. As a result the region boundaries in their approach remained sharp and yielded a good quality edge detector.

A manifold of diffusion coefficients have been studied and showed upgraded results in enhancing the image. An Honorable mention goes to Blanc-Feraud et al [11]. However, all of these upgrades shared a common serious point. None proposed an optimal value of λ and only relied on computational result to determine a value. This is a subject matter which shall be discussed shortly hereafter.

In parallel, the equation was subject to many critics. Most were very positive as the equation over passed what was then considered standard expectations. However, some were negatively serious and showed some drawbacks of the nonlinear anisotropic operator. Namely, Voci et al in [60] pointed out that the equation is not stable and that the generated solution is not necessarily regular. Also, and despite the good quality edge detector, sharp edges and fine details are still not well preserved.

To overcome these flaws, numerous suggestions were put forward. For instance, Black et al.[10] proposed an optimal value of λ which showed a significant upgrade to image filtering. The value is obtained through statistical interpretation and is equal to

$$\lambda = 1.4826\,\mathrm{MAD}(\nabla u)/\sqrt{2},$$

where $\mathrm{MAD}\,(\nabla u) = \mathrm{median}_u\,|\nabla u - \mathrm{median}_u\,(|\nabla u|)\,|$ and $\mathrm{median}_u\,|\nabla u|$ represents the median over the image u of the gradient amplitude. The statistical value allowed for the detection of edges between piecewise smooth regions in an image smoothed using anisotropic diffusion. Making the algorithm more powerful in detecting noncontinuous noise.

Another approach dealt with deploying a Gaussian filter to the gradient (see Catté et al.[13]) yielding the equation

$$\begin{cases} \partial_t u - \mathrm{div}\left(g\left(\left|G_\sigma * \nabla u\right|, \lambda\right)\nabla u\right) = 0 & \text{in } Q_T \\ u(0,x) = u_0(x) & \text{in } \Omega \\ \dfrac{\partial u}{\partial \nu} = 0 & \text{on } \Sigma_T, \end{cases}$$

where $G_\sigma(x) = \frac{1}{2\pi\sigma^2}\exp\left(-\frac{|x|^2}{2\sigma^2}\right)$ denotes the Gaussian Kernel. By doing so, the equation became well posed and achieved a relatively better filtering. The parameter λ, in fact, may discriminate between areas with the lowest and maximum image gradients. Image areas where $|G_\sigma * \nabla u| < \lambda$ are regarded as uniform regions where noise must be decreased. The diffusion function then holds high values. Parts of the image where $|G_\sigma * \nabla u| \geq \lambda$, conversly, are classified brutal changes of intensity caused by the contours and thus must be retained. The function of diffusivity takes values virtually zero, impeding diffusion. The algorithm is also shown to be stable see the works[28,41].

Other researches included a nonlinear function to the equation allowing both filtering and contrast enhancement of the image all while keeping the equation well posed. Take for instance Morfu's[46] algorithm which reads

$$\begin{cases} \partial_t u - \mathrm{div}(g(|\nabla u|, \lambda)\nabla u) = f(u) & \text{in } Q_T \\ u(0,x) = u_0(x) & \text{in } \Omega \\ \dfrac{\partial u}{\partial \nu} = 0 & \text{on } \Sigma_T, \end{cases}$$

where $f(\cdot)$ is a nonlinear function with the sole objective to moderate the weight of the nonlinearity in the equation. It was framed so that it tends to 0 if the algorithm deals with continuous noise (the equation is then equivalent to that of Perona-Malik's which showed excellent results in filtering continuous noise) or to ensure a sense of symmetry while dealing with discontinuous noise.

Some researchers even went to the extent of combining all previous approaches in a one single algorithm. Namely, Alaa et al.'s[2] equation is written

$$\begin{cases} \partial_t u - \mathrm{div}\left(g\left(\left|G_\sigma * \nabla u\right|, \lambda\right)\nabla u\right) = f(u) & \text{in } Q_T \\ u(0,x) = u_0(x) & \text{in } \Omega \\ \dfrac{\partial u}{\partial \nu} = 0 & \text{on } \Sigma_T, \end{cases}$$

Their choice of the functional $g(\cdot)$ was that of Charbonnier et al[14]

$$g(|\nabla u|, \lambda) = \frac{d}{\left(1 + \left(\frac{|\nabla u|}{\lambda}\right)^2\right)^{\frac{1}{2}}},$$

which was shown to provide more regularization compared to its peers. The parameter d is a non-negative constant. The nonlinearity $f(\cdot)$ was a customarily choice by Nagumo et al[47] and FitzHugh[26] equivalent to

$$f(u) = -\beta u(u-\alpha)(u-1),$$

the parameter β plays the role of a moderator. It will tend to 0 around continuous noise. The parameter α is the threshold ensuring the symmetry of the nonlinearity around discontinuous noise. The authors showed that the equation is well posed, stable and more importantly inherits all the strengths of the previous models as it contains protocols to separate continuous noise and discontinuous noise, a protocol to differentiate edges and contours to avoid applying diffusion on such areas and robust mathematical build[5].

All mentioned above are Perona-Malik diffusion based methods which rely on regularization. Another genre are TV-based approaches[38] which avail of optimization techniques. They lead to a relatively rapid and factual solution. One may say they are simply stronger. However, TV-based denoising is keen to piecewise constant functions solutions. Aside from that, it sometimes causes what we call a staircasing effect. Piecewise constant regions are created from noisy smooth portions in the image, resulting in false edges. This generally means misinterpretation of image features by the machine. This was repeatedly observed in the

literature (see[20] and many references therein). To overcome this shortcoming, researchers designed a regularizing term. Rhetorically speaking, they generalized the techniques mentioned above to take advantage of each's strengths. The original version of this approach was proposed by Chen et al[19]. It is based on an anisotropic reaction-diffusion equation with variant exponent which reads

$$\begin{cases} \partial_t u - \operatorname{div}(\phi(x, \nabla u)) = \theta(u_0 - u) & \text{in } Q_T \\ u(0, x) = u_0(x) & \text{in } \Omega \\ \dfrac{\partial u}{\partial \nu} = 0 & \text{on } \Sigma_T, \end{cases}$$

where $\phi(x, r) := \begin{cases} \frac{1}{p(x)}|r|^{p(x)}, & |r| \le \delta \\ |r| - \frac{\delta p(x) - \delta^{p(x)}}{p(x)}, & |r| > \delta \end{cases}$ represents the regularizing term.

A typical choice of the functional $p(\cdot)$ reads

$$p(x) = 1 + \frac{1}{1 + k|\nabla G_\sigma * u_0(x)|^2},$$

where $k > 0$, $\delta > 0$ and $\theta > 0$ are fixed constants which we will discuss in the next lines.

Notice that where the gradient is near zero (inhomogeneous regions), the model is isotropic. When the gradient is large enough (presumably at the edges), only TV-model diffusion will be used. At all other locations, the filtering is medially between Gaussian and TV-based diffusion. The option to how accommodates local image information is what made this model very powerful and solid inspiration for many subsequent works. Let's call it the *picker* for the sake of our argument to be found down the lines. This option is directly related to the choice of the parameter δ. Its value is handpicked. Intuitively. Often by comparing various numerical thresholds. This suggested room for improvement. Many efforts had been made to optimize this choice (see[36,58] and many references therein).

One of the approaches has been established by Guo et al[30] which is inspired from the work of Osher et al[48] and Strong et al[56] alongside the above PDE by Chen et al[19]. It uses anisotropic reaction-diffusion systems with $p(x)$-growth which read

$$\begin{cases} \partial_t u - \operatorname{div}\left(\mathcal{G}(x)|\nabla u|^{p(x)-2}\nabla u\right) = -2\lambda v & \text{in } Q_T \\ \partial_t v - \Delta v = u - u_0 & \text{in } Q_T \\ u(0, x) = u_0(x), \quad v(0, x) = 0 & \text{in } \Omega \\ \dfrac{\partial u}{\partial \nu} = \dfrac{\partial v}{\partial \nu} = 0 & \text{in } \Sigma_T, \end{cases}$$

where

$$\mathcal{G}(x) = \frac{1}{1 + k_1|\nabla G_{\sigma_1} * u_0(x)|^2} \quad \text{and} \quad p(x) = 1 + \frac{1}{1 + k_2|\nabla G_{\sigma_2} * u_0(x)|^2},$$

here k_1, k_2, σ_1 and σ_2 are fixed nonnegatives constants. Both terms $\mathcal{G}(\cdot)$ and $p(\cdot)$ depend on the location x. This means that local behavior determines the direction and speed of diffusion at each location. Opposite to the gradient, the term $\mathcal{G}(\cdot)$ is relatively larger on homogeneous regions than in edges (nonhomogeneous regions). A smoothing effect is then created near the edges by the diffusion in the first line of the above systems or what we call the denoising equation. The main feature is the nonlinearity's adaptability, which results in a gap between homogeneous and non-homogeneous regions. This is more detailed in their paper.

As to how these models work, the denoising equation allows the construction of a smooth image u. The fidelity term v is computed differently and is used to minimize the differences between the main features of the noisy image u_0 and the smooth image u.

1.1 | Proposed model

We shall introduce a novel model to address the challenge. We are concerned with a nonlinear parabolic equation with variable growth conditions modeled as

$$\begin{cases} \partial_t u - \operatorname{div}\left(g(|\nabla u_\sigma|, \lambda)|\nabla u|^{p(x)-2}\nabla u\right) = f(t, x, u) & \text{in } Q_T \\ u(0, x) = u_0(x) & \text{in } \Omega \\ u = 0 & \text{on } \Sigma_T, \end{cases} \tag{1}$$

where the initial data u_0 is assumed to be a measurable function belonging in $L^2(\Omega)$, $f : Q_T \times \mathbb{R} \to \mathbb{R}$ is a Carathéodory function satisfying some assumptions to be specified latter and $p(\cdot)$ is a continuous function on $\overline{\Omega}$ such that $\inf_{x\in\overline{\Omega}} p(x) > 1$. The

anisotropic diffusivity coefficient $g(\cdot)$ is assumed to be a smooth non-increasing function such that $g(0,\lambda)=1$ and $\lim_{s\to\infty} g(s,\lambda)=0$. For simplicity reasons, we will denote by $g(\cdot)$ the diffusivity coefficient instead of $g(\cdot,\lambda)$. Furthermore, we will give explicitly our choice of $g(\cdot)$ in Section 5.

To itemize, the first strength of our model relies on being an optimized tool to accommodate local image information. Whilst Chen's *picker* relies on the manual choice of δ to differentiate the application of the isotropic operator or TV-based diffusion as explained above, our *picker* is a smart mechanism that adapts to local information and is more optimal than that of Guo's model. To explain, opposite to the gradient, the term $g(|\nabla u_\sigma|)$ is relatively larger on homogeneous regions than on edges. A smoothing effect similar to that of Guo's model is then created near the edges by the diffusion. Even more, the main feature of our *picker* is the adaptation character of the nonlinearity. It plays the role of the parameter δ in Chen's equation as it ensures TV-model diffusion (when p goes to 1) along the non-homogeneous edges and Gaussian smoothing (when p goes to 2) in homogeneous areas.

To put it in simple words, our design simply avoids manually picking *the picker* and goes to the extent of choosing the optimal possible value by interpreting local image information. Our model also have a very important feature: It tackles a wider range of equations of this alike. Notice that it generalizes all previous equations under one simple line. The anisotropic diffusivity coefficient and the variable exponent are no longer restricted to specific options. In fact, we only assume that the variable exponent $p(\cdot)$ is a continuous function on $\overline{\Omega}$ with $\inf_{x\in\overline{\Omega}} p(x) > 1$. Also, the nonlinearity $f(\cdot)$ may depend on time seizing more range. Even more importantly, we shall prove that only relatively weak growth conditions are required to the existence of a weak solution of the equation (1). The latter is one of the main results of this work.

1.2 | Paper outline

We have structured our paper as follows. In Section 2, we put forward the mathematical tools required for the study of our equation as well as the definition of its weak solution. In Section 3, we acquire the first theoretical result concerning the existence of a weak solution under the assumption of bounded nonlinearity. In Section 4, we establish an approximate problem of our equation and we deploy the existence result of Section 3 to prove the existence of a weak solution with no growth restrictions on the nonlinearity. Section 5 is devoted to discretizing the proposed model (1) into the numerical framework. We will start by giving our choice to the input functions $p(\cdot)$, $g(\cdot)$ and $f(\cdot)$. Thereafter, we detail the computation process of our model. Section 6 casts numerical simulations validating our theoretical results.

2 | MATHEMATICAL BACKGROUNDS AND ASSUMPTIONS

As well known, theoretical analysis of PDEs involving $p(x)$-growth conditions need the use of some complex spaces called Lebesgue and Sobolev spaces with variable exponents (see for example[3,7,16,17,24,32,40,52,53]). Therefore, the variable exponent $p(\cdot)$ appears in problem (1) requires the consideration of these types of spaces. For the reader's convenience, we shall start by recalling some definitions, useful relationships, and properties of such spaces. And for a complete presentation about these spaces, we refer the interesting readers to Antontsev and Shmarev[6], Diening et al[22] and Rădulescu and Repovš[51].

2.1 | Lebesgue and Sobolev spaces with variable exponent

For a given $p\in C\left(\overline{\Omega}\right)$, we define a couple of real values $\left(p^-,p^+\right)$ as

$$p^- = \inf_{x\in\overline{\Omega}} p(x) \quad \text{and} \quad p^+ = \sup_{x\in\overline{\Omega}} p(x).$$

We set

$$\mathcal{E}_1 := \left\{ p\in C\left(\overline{\Omega}\right) \,:\, p^- > 1 \right\}, \qquad \mathcal{M}(\Omega) := \{u : \Omega \to \mathbb{R} \text{ measurable}\}.$$

We define the variable exponent Lebesgue space $L^{p(x)}(\Omega)$ as follows

$$L^{p(x)}(\Omega) = \left\{ u\in\mathcal{M}(\Omega) \,:\, \rho_{p(x)}(u) < \infty \right\}.$$

where $\rho_{p(\cdot)}$ designates the following convex modular

$$\rho_{p(x)}(u) = \int_{\Omega} |u(x)|^{p(x)} dx.$$

The space $L^{p(x)}(\Omega)$ is eqquiped by the so-called Luxemburg norm

$$\|u\|_{p(x)} = \inf \left\{ \mu > 0, \quad \rho_{p(x)}\left(\frac{u}{\mu}\right) \leq 1 \right\}.$$

When $p(\cdot) \in \mathcal{E}_1$, the space $(L^{p(x)}(\Omega), \|\cdot\|_{p(x)})$ comes to be a separable, reflexive Banach space. Moreover, for any $p(\cdot) \in \mathcal{E}_1$, we denote by $p'(x) = \frac{p(x)}{p(x)-1}$ the conjugate exponent of $p(x)$ and therefore, we can define $L^{p'(x)}(\Omega)$ as the dual space of $L^{p(x)}(\Omega)$. In the following proposition, we state interesting inequalities which are known by $p(x)$-Hölder inequalities.

Proposition 1. Let $p(\cdot) \in \mathcal{E}_1$. For any $u \in L^{p(x)}(\Omega)$ and $v \in L^{p'(x)}(\Omega)$, we have

$$\left| \int_{\Omega} uv\, dx \right| \leq \left(\frac{1}{p^-} + \frac{1}{(p^-)'} \right) \|u\|_{p(x)} \|v\|_{p'(x)} \leq 2\|u\|_{p(x)} \|v\|_{p'(x)}.$$

Moreover, if $\frac{1}{p(x)} + \frac{1}{p'(x)} + \frac{1}{p''(x)} = 1$, then

$$\left| \int_{\Omega} uvw\, dx \right| \leq \left(\frac{1}{p^-} + \frac{1}{(p^-)'} + \frac{1}{(p^-)''} \right) \|u\|_{p(x)} \|v\|_{p'(x)} \|w\|_{p''(x)} \leq 3\|u\|_{p(x)} \|v\|_{p'(x)} \|w\|_{p''(x)},$$

for all $u \in L^{p(x)}(\Omega)$, $v \in L^{p'(x)}(\Omega)$ and $w \in L^{p''(x)}(\Omega)$.

By the same way, we define the variable exponent Lebesgue space $L^{p(x)}(Q_T)$ as follows

$$L^{p(x)}(Q_T) = \left\{ u \in \mathcal{M}(Q_T) \ : \ \int_{Q_T} |u(t,x)|^{p(x)} dx\, dt < \infty \right\}.$$

We equip $L^{p(x)}(Q_T)$ with the following norm

$$\|u\|_{p(x)} = \inf \left\{ \mu > 0, \ \int_{Q_T} \left| \frac{u(t,x)}{\mu} \right|^{p(x)} dx\, dt \leq 1 \right\}.$$

If $p(\cdot) \in \mathcal{E}_1$, the space $\left(L^{p(x)}(Q_T), \|\cdot\|_{p(x)}\right)$ becomes a separable, reflexive Banach space. Now, we introduce the Sobolev space with variable exponent $W^{1,p(x)}(\Omega)$ such as

$$W^{1,\,p(x)}(\Omega) = \left\{ u \in L^{p(x)}(\Omega), \quad |\nabla u| \in L^{p(x)}(\Omega) \right\}.$$

We consider on $W^{1,p(x)}(\Omega)$ the following norm

$$\|u\|_{1,\,p(x)} = \|u\|_{p(x)} + \|\nabla u\|_{p(x)}.$$

Which is equivalent to

$$\|u\|_{1,p(x)} = \inf \left\{ \mu > 0, \int_{\Omega} \left(\left| \frac{\nabla u(x)}{\mu} \right|^{p(x)} + \left| \frac{u(x)}{\mu} \right|^{p(x)} \right) dx \leq 1 \right\}.$$

In what follows, we assume that $p(\cdot)$ meets the log-Hölder continuity condition which states that there exists a nonnegative constant C such that

$$|p(x_1) - p(x_2)| \leq \frac{-C}{log|x_1 - x_2|}, \forall x_1, x_2 \in \Omega, \ \text{ with } \ |x_1 - x_2| < \frac{1}{2}. \tag{2}$$

When $p(\cdot) \in \mathcal{E}_1$ sataisfies the assumption (2), the space $C_c^{\infty}(\Omega)$ of smooth functions is dense in the Sobolev space $W^{1,p(x)}(\Omega)$. We define the Dirichlet anisotropic Sobolev space

$$W_0^{1,p(x)}(\Omega) := \overline{C_c^{\infty}(\Omega)}^{W^{1,p(x)}(\Omega)}.$$

We designate by $\left(W_0^{1,p(x)}(\Omega)\right)^*$ the dual space of $W_0^{1,p(x)}(\Omega)$. As a result, the Sobolev spaces $W^{1,p(x)}(\Omega)$ and $W_0^{1,p(x)}(\Omega)$ are separable and reflexive Banach spaces. An interesting feature result is the following $p(x)$-Poincaré inequality, for any $u \in W_0^{1,p(x)}(\Omega)$ we have

$$\|u\|_{p(x)} \leq C\|\nabla u\|_{p(x)}.$$

where C is a nonnegative constant depending only on Ω and $p(\cdot)$. In view to the $p(x)$-Poincaré inequality, we can consider $\|\nabla u\|_{p(x)}$ as a norm on $W_0^{1,p(x)}(\Omega)$. We describe several noteworthy properties of Lebesgue and Sobolev spaces with variable exponents in the following assertions.

Proposition 2.

1. For any $u \in L^{p(x)}(\Omega)$, we have the following relationships

$$\min\left\{\|u\|_{p(x)}^{p^-}, \|u\|_{p(x)}^{p^+}\right\} \leq \rho_{p(x)}(u) \leq \max\left\{\|u\|_{p(x)}^{p^-}, \|u\|_{p(x)}^{p^+}\right\}. \tag{3}$$

$$\min\left\{\rho_{p(x)}^{\frac{1}{p^-}}(u), \rho_{p(x)}^{\frac{1}{p^+}}(u)\right\} \leq \|u\|_{p(x)} \leq \max\left\{\rho_{p(x)}^{\frac{1}{p^-}}(u), \rho_{p(x)}^{\frac{1}{p^+}}(u)\right\}. \tag{4}$$

2. Let (u_n) be a sequence in $L^{p(x)}(\Omega)$, then the following statements are equivalent:

   (i) $\lim\limits_{n\to+\infty} \|u_n - u\|_{L^{p(x)}(\Omega)} = 0.$

   (ii) $\lim\limits_{n\to+\infty} \rho_{p(x)}\left(u_n - u\right) = 0.$

   (iii) $u_n \to u$ in measure in Ω and $\lim\limits_{n\to+\infty} \rho_{p(x)}\left(u_n\right) = \rho_{p(x)}(u).$

Proposition 3.

1. Let $p_1(\cdot), p_2(\cdot) \in \mathcal{E}_1$ such that $p_1(x) \leq p_2(x)$ almost everywhere in Ω. Then, we have the continuous embedding $L^{p_2(x)}(\Omega) \hookrightarrow L^{p_1(x)}(\Omega)$.

2. Let $p(\cdot), q(\cdot) \in \mathcal{E}_1$ such that $1 \leq q(x) < p^*(x)$, for all $x \in \overline{\Omega}$, then the embedding $W_0^{1,p(x)}(\Omega) \hookrightarrow L^{q(x)}(\Omega)$ is continuous and compact, where

$$p^*(x) := \begin{cases} \frac{Np(x)}{N-p(x)}, & p(x) < N \\ +\infty, & p(x) \geq N. \end{cases}$$

2.2 | Assumptions

Throughout this paper, we assume that $p(\cdot) \in \mathcal{E}_1$ satisfies the log-Hölder continuity condition (2). In addition, we present here the main hypothesis on the nonlinearity f. We assume that

$(\mathcal{H}_1)$ $f : Q_T \times \mathbb{R} \to \mathbb{R}$ is a Carathéodory function, namely

$$s \mapsto f(t,x,s) \text{ is continuous for a.e } (t,x) \in Q_T, \tag{5}$$

$$(t,x) \mapsto f(t,x,s) \text{ is measurable for all } s \in \mathbb{R}. \tag{6}$$

$(\mathcal{H}_2)$ the positivity property is preserved over time in the following sens:

$$f(t,x,0) \geq 0 \quad \text{for almost } (t,x) \in Q_T. \tag{7}$$

$(\mathcal{H}_3)$ the total mass is controlled with respect to the time

$$f(t,x,s).s \leq 0 \quad \text{for all } s \in \mathbb{R}, \text{ and for almost } (t,x) \in Q_T. \tag{8}$$

$(\mathcal{H}_4)$ f enjoys the following regularity property

$$\sup_{|s|\leq k} |f(t,x,s)| = h_k(t,x) \in L^1(Q_T) \quad \text{for every } k \in \mathbb{R}^+. \tag{9}$$

2.3 | Functional framework and definitions

Now, we are ready to introduce our used functional framework to solve (1). For any $0 < T < +\infty$, we start by introducing the following time space

$$L^{p^-}\left(0,T;W_0^{1,p(x)}(\Omega)\right) := \left\{ u \in L^{p(x)}(Q_T) \,:\, \int_0^T \|\nabla u\|_{p(x)}^{p^-} dt < \infty \right\}.$$

endowed with the norm

$$\|u\|_{L^{p^-}\left(0,T;W_0^{1,p(x)}(\Omega)\right)} = \left(\int_0^T \|\nabla u\|_{p(x)}^{p^-} dt \right)^{\frac{1}{p^-}}.$$

We define the functional space $\mathcal{V}$ which is often used in the theoretical analysis of PDEs with $p(x)$-growth conditions.

$$\mathcal{V} = \left\{ u \in L^{p^-}\left(0,T;W_0^{1,p(x)}(\Omega)\right) \,:\, |\nabla u| \in L^{p(x)}(Q_T) \right\},$$

endowed with the norm

$$\|u\|_{\mathcal{V}} = \|\nabla u\|_{L^{p(x)}(Q_T)}.$$

According to $p(x)$-Poincaré inequality and by the mean of the embedding $L^{p(x)}(Q_T) \hookrightarrow L^{p^-}\left(0,T;L^{p(x)}(\Omega)\right)$, we can cheke that $\|\cdot\|_{\mathcal{V}}$ is equivalent to the following norm

$$|||u||| = \|u\|_{L^{p^-}\left(0,T;W_0^{1,p(x)}(\Omega)\right)} + \|\nabla u\|_{L^{p(x)}(Q_T)}.$$

In view of Lebesgue and Sobolev space with variable exponent, we can easily verify that $\mathcal{V}$ is a Banach space, separable and reflexive. In the sequel, we will denote by $\mathcal{V}^*$ the dual space of. Some interesting properties of the space $\mathcal{V}$ are stated in the following lemma.

Lemma 1 ([12]). Let $\mathcal{V}$ be the space defined as above. Then,

i) we have the following continuous dense embedding

$$L^{p^+}\left(0,T;W_0^{1,p(x)}(\Omega)\right) \hookrightarrow \mathcal{V} \hookrightarrow L^{p^-}\left(0,T;W_0^{1,p(x)}(\Omega)\right). \tag{10}$$

In particular, since $C_c^\infty(Q_T)$ is dense in $L^{p^+}(0,T;W_0^{1,p(x)}(\Omega))$, it is dense in $\mathcal{V}$ and for the corresponding dual spaces we have

$$L^{(p^-)'}\left(0,T;(W_0^{1,p(x)}(\Omega))^*\right) \hookrightarrow \mathcal{V}^* \hookrightarrow L^{(p^+)'}\left(0,T;(W_0^{1,p(x)}(\Omega))^*\right). \tag{11}$$

ii) Moreover, the elements of $\mathcal{V}^*$ are represented as follow: For all $\zeta \in \mathcal{V}^*$, there exists $\xi = \left(\xi_1,\dots,\xi_N\right) \in (L^{p'(x)}(Q_T))^N$ such that: $\zeta = \operatorname{div}(\xi)$ and

$$< \zeta, \varphi >_{\mathcal{V}^*,\mathcal{V}} = \int_{Q_T} \xi \nabla\varphi \, dx \, dt,$$

for any $\varphi \in \mathcal{V}$. Furthermore, we have

$$\|\zeta\|_{\mathcal{V}^*} = max\left\{ \|\xi_i\|_{L^{p(x)}(Q_T)}, i = 1,...,N \right\}.$$

iii) For any $u \in \mathcal{V}$ the following relationship holds true

$$\min\left\{ \|u\|_{\mathcal{V}}^{p^-}, \|u\|_{\mathcal{V}}^{p^+} \right\} \le \int_{Q_T} |\nabla u|^{p(x)} \, dxdt \le \max\left\{ \|u\|_{\mathcal{V}}^{p^-}, \|u\|_{\mathcal{V}}^{p^+} \right\}. \tag{12}$$

Hence, we are ready to define the following set

$$\mathcal{W}(Q_T) := \left\{ u \in \mathcal{V} \cap C\left([0,T];L^2(\Omega)\right) \,:\, \partial_t u \in \mathcal{V}^* \right\}.$$

We will equip it with the graph norm defined by

$$\|u\|_{\mathcal{W}(Q_T)} := \|u\|_{\mathcal{V}} + \|\partial_t u\|_{\mathcal{V}^*}.$$

3 | AN EXISTENCE RESULT FOR ANY BOUNDED REACTION TERM

This section treats a plainer matter of problem (1). That is when the nonlinearity $f(\cdot)$ is bounded by a nonnegative constant. We will prove in Theorem 1 the existence of a weak solution for such case. The result shall serve as a first step into establishing the main result of this manuscript, of which the model of the demonstration is rather conventional, yet very technical. This will be detailed in Section 4.

Theorem 1. Under the hypothesis $(\mathcal{H}_1)$, we assume the existence of a nonnegative constant $\mathbb{M}_f$ such that

$$|f(t,x,s)| \leq \mathbb{M}_f, \quad \text{for all } s \in \mathbb{R}, \text{ and for almost } (t,x) \in Q_T. \tag{13}$$

Then for every $u_0 \in L^2(\Omega)$, problem (1) has a weak solution u in the following sense

$$\begin{gathered} u \in \mathcal{W}(Q_T), \quad u(0) = u_0 \text{ in } L^2(\Omega) \\ \int_0^T \langle \partial_t u, \phi \rangle \, dt + \int_{Q_T} g(|\nabla u_\sigma|) |\nabla u|^{p(x)-2} \nabla u \nabla \phi \, dxdt = \int_{Q_T} f(t,x,u)\phi \, dxdt \end{gathered} \tag{14}$$

for all test function $\phi \in \mathcal{V}$.

Remark 1. Thanks to assumption (13), we know that all the terms of (14) are well defined. In fact for all $u \in \mathcal{V}$ we have $f(t,x,u)$ belongs to $L^{(p^-)'}(Q_T)$. Hence, we justify that $f(t,x,u)\phi$ belongs to $L^1(Q_T)$ for all $\phi \in \mathcal{V}$.

Proof. To prove the result of Theorem 1, we propose to use Schauder fixed point theorem. We start initially by reformulating the question about the existence of a weak solution to problem (1) into the research of a fixed point to a well-posed mapping. Let $v \in \mathcal{W}(Q_T)$, we consider the following linearized problem

$$\begin{cases} \partial_t u - \operatorname{div}\left(g(|\nabla v_\sigma|)|\nabla u|^{p(x)-2}\nabla u\right) = f(t,x,v) & \text{in } Q_T \\ u(0,x) = u_0(x) & \text{in } \Omega \\ u(t,x) = 0 & \text{on } \Sigma_T. \end{cases} \tag{15}$$

It is worth mentioning that the gaussian function G_σ is belonging in $C^\infty(\Omega)$, which leads to obtain that $|G_\sigma * v|$ is belonging in $L^\infty(0,T;C^\infty(\Omega))$. On the other hand, by applying the fact that $g(\cdot)$ is non-increasing, one may deduce the existence of $\alpha,\ \beta > 0$ a positive constants which deponding only on σ, $g(\cdot)$ and $\|u_0\|_{L^2(\Omega)}$ such that

$$\alpha \leq g(|\nabla v_\sigma|) \leq \beta, \tag{16}$$

for all $v \in \mathcal{W}(Q_T)$. By the classical methods (for instance, the difference and variation methods from [61] or the monotone operator theory in [37,42,54]), one may deduce that for a fixed $v \in \mathcal{W}(Q_T)$, problem (15) has a unique weak solution u which satisfies the following weak formulation

$$u \in \mathcal{W}(Q_T), \quad u(0) = u_0 \text{ in } L^2(\Omega) \tag{17}$$

$$\int_0^T \langle \partial_t u, \phi \rangle \, dt + \int_{Q_T} g(|\nabla v_\sigma|) |\nabla u|^{p(x)-2} \nabla u \nabla \phi \, dxdt = \int_{Q_T} f(t,x,v)\phi \, dxdt \tag{18}$$

for all test function $\phi \in \mathcal{V}$. As a consequence, the mapping $v \in \mathcal{W}(Q_T) \to u \in \mathcal{W}(Q_T)$ is well-defined. As we know, to apply the Schauder fixed point we need to build a functional framework that involves our result. To do this, we shall prove some interesting *a prior estimates*. Let us consider $\phi = u\chi_{(0,t)}$ as a test function in the weak formulation (18) such that $0 < t < T$. We get

$$\frac{1}{2}\int_\Omega u^2(t)\, dx + \int_{Q_t} g(|\nabla v_\sigma|)|\nabla u|^{p(x)} \, dxdt = \frac{1}{2}\int_\Omega u_0^2 \, dx + \int_{Q_t} f(t,x,v)u \, dxdt, \tag{19}$$

where $Q_t = (0,t)\times\Omega$. By applying (16) the equation (19) becomes

$$\frac{1}{2}\int_\Omega u^2(t)\, dx + \alpha \int_{Q_t} |\nabla u|^{p(x)} \, dxdt \leq \frac{1}{2}\int_\Omega u_0^2 \, dx + \int_{Q_t} |f(t,x,v)u| \, dxdt. \tag{20}$$

Thanks to assumption (13), we obtain

$$\int_{\Omega} u^2(t)\,dx \le \int_{Q_t} \mathbb{M}_f^2\,dxdt + \int_{Q_t} u^2\,dxdt + \int_{\Omega} u_0^2\,dx. \tag{21}$$

With the help of Gronwall's lemma, we arrive at

$$\int_{Q_T} u^2\,dxdt \le (\exp(T)-1)\left(T\mathbb{M}_f^2\,\mathrm{meas}(\Omega) + \int_{\Omega} u_0^2\,dx\right). \tag{22}$$

Substituting the result of (22) in (21), one gets

$$\|u\|_{L^\infty(0,T;L^2(\Omega))} \le \exp(T)\left(T\mathbb{M}_f^2\,\mathrm{meas}(\Omega) + \|u_0\|^2_{L^2(\Omega)}\right). \tag{23}$$

On the other hand, using (12), (20) and (22), we deduce that

$$\min\left\{\|u\|_{\mathcal{V}}^{p^-}, \|u\|_{\mathcal{V}}^{p^+}\right\} \le \frac{\exp(T)}{\alpha}\left(T\mathbb{M}_f^2\,\mathrm{meas}(\Omega) + \|u_0\|^2_{L^2(\Omega)}\right). \tag{24}$$

From (23) and (24), we know that

$$\|u\|_{L^\infty(0,T;L^2(\Omega))} + \min\left\{\|u\|_{\mathcal{V}}^{p^-}, \|u\|_{\mathcal{V}}^{p^+}\right\} \le C_1. \tag{25}$$

where C_1 is a constant depending on $\alpha, \mathbb{M}_f, T, \Omega$ and u_0. Furthermore, for any $\phi \in \mathcal{V}$, we have

$$\left|\left\langle -\mathrm{div}\left(g(|\nabla v_\sigma|)|\nabla u|^{p(x)-2}\nabla u\right), \phi\right\rangle\right| = \left|\int_{Q_T} g(|\nabla v_\sigma|)|\nabla u|^{p(x)-2}\nabla u\nabla\phi\,dxdt\right| \le \beta\int_{Q_T} |\nabla u|^{p(x)-1}\,|\nabla\phi|\;dxdt.$$

Employing $p(x)$-Hölder inequality, we obtain

$$\begin{aligned}\left|\left\langle -\mathrm{div}\left(g(|\nabla v_\sigma|)|\nabla u|^{p(x)-2}\nabla u\right), \phi\right\rangle\right| &\le C\|\,|\nabla u|^{p(x)-1}\,\|_{L^{p'(x)}(Q_T)}\|\nabla\phi\|_{L^{p(x)}(Q_T)}\\ &\le C\|\,|\nabla u|^{p(x)-1}\,\|_{L^{p'(x)}(Q_T)}\|\phi\|_{\mathcal{V}}.\end{aligned} \tag{26}$$

On the other hand, the result of Proposition 2 implies

$$\begin{aligned}\|\,|\nabla u|^{p(x)-1}\|_{L^{p'(x)}(Q_T)} &\le \max\left\{\left(\int_{Q_T}|\nabla u|^{p(x)}\right)^{\frac{1}{(p')^-}}, \left(\int_{Q_T}|\nabla u|^{p(x)}\right)^{\frac{1}{(p')^+}}\right\}\\ &\le \max\left\{\|\nabla u\|^{\frac{p^+}{(p')^-}}_{L^{p(x)}(Q_T)}, \|\nabla u\|^{\frac{p^+}{(p')^+}}_{L^{p(x)}(Q_T)}\right\}\\ &\le C\max\left\{\|u\|_{\mathcal{V}}^{\frac{p^+}{(p')^-}}, \|u\|_{\mathcal{V}}^{\frac{p^+}{(p')^+}}\right\},\end{aligned} \tag{27}$$

where C is a constant depends only on p^-, p^+ and Ω. From (26), (27) and (24), we deduce that

$$\left|\left\langle -\mathrm{div}\left(g(|\nabla v_\sigma|)|\nabla u|^{p(x)-2}\nabla u_n\right), \phi\right\rangle\right| \le C\left(\alpha, \beta, p^-, p^+, T, \Omega, u_0\right)\|\phi\|_{\mathcal{V}}. \tag{28}$$

Since

$$\left\|\mathrm{div}\left(g(|\nabla v_\sigma|)|\nabla u|^{p(x)-2}\nabla u\right)\right\|_{\mathcal{V}^*} = \sup_{\phi\in\mathcal{V},\,\|\phi\|_{\mathcal{V}}\neq 0}\frac{\left|\left\langle \mathrm{div}\left(g(|\nabla v_\sigma|)|\nabla u|^{p(x)-2}\nabla u\right), \phi\right\rangle\right|}{\|\phi\|_{\mathcal{V}}}. \tag{29}$$

We know from (28) and (29) that $\left(\mathrm{div}\left(g(|\nabla v_\sigma|)|\nabla u|^{p(x)-2}\nabla u\right)\right)$ is bounded in $\mathcal{V}^*$. Moreover, with the help of assumption (13) and by taking into account the equation satisfied by u, we conclude that

$$\|\partial_t u\|_{\mathcal{V}^*} \le C_2, \tag{30}$$

where C_2 is a constant depending on $\alpha, \beta, \mathbb{M}_f, T, \Omega$ and u_0. By arguing the estimates (23) and (30) we are able to construct the following space

$$\mathbb{W}(Q_T) := \left\{u \in \mathcal{W}(Q_T)\ :\ \|u\|_{L^\infty(0,T;L^2(\Omega))} + \min\left\{\|u\|_{\mathcal{V}}^{p^-}, \|u\|_{\mathcal{V}}^{p^+}\right\} \le C_1, \|\partial_t u\|_{\mathcal{V}^*} \le C_2,\, u(0) = u_0\right\}.$$

It is clearly that $\mathbb{W}(Q_T)$ is a nonempty closed convex in $\mathcal{W}(Q_T)$. Then, we consider the following mapping

$$\begin{aligned} \mathcal{F} : \mathbb{W}(Q_T) &\longrightarrow \mathbb{W}(Q_T) \\ v &\longmapsto u \end{aligned}$$

where u is the unique weak solution to the problem (15). In order to apply Schauder fixed point theorem, we shall establish that the mapping $\mathcal{F}$ is weakly continuous on the space $\mathbb{W}(Q_T)$. To do this, we consider (v_n) a sequence in $\mathbb{W}(Q_T)$ such that

$$(v_n) \to v \text{ weakly in } \mathbb{W}(Q_T). \tag{31}$$

We will prove that $\mathcal{F}(v_n)$ converges weakly to $\mathcal{F}(v)$ in $\mathbb{W}(Q_T)$. To do this, we set $u_n = \mathcal{F}(v_n)$. It is clear that (u_n) is a weak solution to the following equation

$$\begin{cases} \partial_t u_n - \operatorname{div}\left(g(|\nabla(v_n)_\sigma|)|\nabla u_n|^{p(x)-2}\nabla u_n\right) = f(t,x,v_n) & \text{in } Q_T \\ u_n(0,x) = u_0(x) & \text{in } \Omega \\ u_n(t,x) = 0 & \text{on } \Sigma_T. \end{cases} \tag{32}$$

According to the above estimates, we know that (u_n, v_n) are bounded in $\mathcal{V}\times\mathcal{V}$ and $\left(\partial_t u_n, \partial_t v_n\right)$ are bounded in $\mathcal{V}^*\times\mathcal{V}^*$. Using the compactness results of Lemma 5.2 from[15], we derive the existence of a subsequence of (u_n, v_n) which will be denoted again (u_n, v_n) for simplicity such that

$$\begin{aligned} (u_n, v_n) &\to (u, v) \text{ strongly in } L^{p^-}(Q_T)\times L^{p^-}(Q_T) \text{ and a.e. in } Q_T, \\ (\nabla u_n, \nabla v_n) &\to (\nabla u, \nabla v) \text{ a.e. in } Q_T. \end{aligned} \tag{33}$$

Using (16), (26), (27) and (33), we can derive the following convergence

$$\left(\nabla G_\sigma * v_n\right) \to \nabla G_\sigma * v \text{ strongly in } L^{p^-}(Q_T) \text{ and a.e. in } Q_T, \tag{34}$$

$$\left(|\nabla u_n|^{p(x)-2}\nabla u_n\right) \rightharpoonup |\nabla u|^{p(x)-2}\nabla u \text{ weakly in } L^{p'(x)}(Q_T). \tag{35}$$

Based on the above estimates and by using the convergences (31), (33), (34) and (35), we get

- $(u_n, v_n) \to (u, v)$ strongly in $L^{p^-}(Q_T)\times L^{p^-}(Q_T)$ and a.e. in Q_T
- $(u_n) \rightharpoonup u$ weakly in $\mathcal{V}$
- $\left(\partial_t u_n\right) \rightharpoonup \partial_t u$ weakly in $\mathcal{V}^*$
- $\left(g(|\nabla(v_n)_\sigma|)|\nabla u_n|^{p(x)-2}\nabla u_n\right) \rightharpoonup g(|\nabla v_\sigma|)|\nabla u|^{p(x)-2}\nabla u$ weakly in $L^{p'(x)}(Q_T)$
- $\left(f(t,x,v_n)\right) \to f(t,x,v)$ strongly in $L^{p'(x)}(Q_T)$.

The latter convergence is obtained with the help of assumption (13) and via Lebesgue's dominated convergence theorem. With the help of the previous convergences, we can pass to the limit in the weak formulation of (32) and establish that the limit u is a solution to (15). Furthermore, using the fact that the solution of (15) is unique, one may deduce that $u = \mathcal{F}(v)$. Which proves that the mapping $\mathcal{F}$ is weakly continuous. According to the Classical Schauder fixed point theory (see e.g[49]), we deduce that the problem (1) has a weak solution u satisfying the weak formulation (14). Which ends the proof of Theorem 1. □

4 | SOLVABILITY OF THE PROPOSED MODEL

In this section, we study the existence of a weak solution to the proposed model (1) under the assumptions $(\mathcal{H}_1)$-$(\mathcal{H}_4)$. It is also worth mentioning that the nonlinearity f has no restriction on the growth. This advantage allows us to include several types of nonlinearities. For example those of non-polynomial type. Before enunciating the main results of our work, we state the definition of weak solution which will be adapted to solve the problem (1).

Definition 1. We call a weak solution to problem (1) all function $u \in \mathcal{M}(Q_T)$ that it satisfies the following properties

$$u \in \mathcal{V}\cap C\left([0,T], L^2(\Omega)\right), \quad f(t,x,u) \in L^1(Q_T)$$

$$-\int_{Q_T} u\partial_t\varphi\, dxdt + \int_{Q_T} g(|\nabla u_\sigma|)|\nabla u|^{p(x)-2}\nabla u\nabla\varphi\, dxdt = \int_\Omega u_0\varphi(0)\, dx + \int_{Q_T} f(t,x,u)\varphi\, dxdt$$

for all $\varphi \in C^1(Q_T)$ with $\varphi(T,\cdot) = 0$.

In the following theorem, we will exhibit the main result of this section.

Theorem 2. Assume that the assumptions $(\mathcal{H}_1)$-$(\mathcal{H}_4)$ hold. Then, for any nonnegative initial condition $u_0 \in L^2(\Omega)$, the problem (1) admits a nonnegative weak solution u which satisfies the conditions of Definition 1.

To prove the existence result of Theorem 2, we propose to work by approximation. So, we are concerned by SOLA solution (a solution obtained as a limit of approximation). We will start by truncate the nonlinearity f to become bounded almost everywhere by a nonnegative constant. After that, we shall define an approximate system to (1). We will assure the existence of a weak solution to the last one via the result of Section 3. Thereafter, we will establish some a priori estimates on the approximate solution. Finally, we use some compactness arguments to pass to the limit in all the terms of the approximate problem.

4.1 | Approximate problem

Let $n > 0$, we approximate the nonlinearities f as follows

$$f_n(t,x,s) = \Psi(|s|) f(t,x,s), \tag{36}$$

where the truncation function $\Psi_n(\cdot) \in C_c^\infty(\mathbb{R})$ defined by

$$\Psi_n(s) = \begin{cases} 1 & \text{if } |s| \le n \\ 0 & \text{if } |s| \ge n+1, \end{cases} \tag{37}$$

and verifies $0 \le \Psi_n(\cdot) \le 1$. It is clear that the functions f_n satisfies the assumptions $(\mathcal{H}_1)$-$(\mathcal{H}_4)$. Moreover, let us remark that by (9) and (36) we have $|f_n| \le \mathbb{M}_f(n)$ where $\mathbb{M}_f(n)$ is a nonnegative which depends only on n. Now, we define an approximate version of the proposed model (1) as follows

$$\begin{cases} \partial_t u_n - \operatorname{div}\left(g(|\nabla(u_n)_\sigma|)|\nabla u_n|^{p(x)-2}\nabla u_n\right) = f_n(t,x,u_n) & \text{in } Q_T \\ u_n(0,x) = u_0(x) & \text{in } \Omega \\ u_n(t,x) = 0 & \text{on } \Sigma_T. \end{cases} \tag{38}$$

Thanks to the result of Theorem 1 from Section 3, we deduce the existence of a weak solution u_n to the approximate problem (38) satisfying

$$u_n \in \mathcal{W}(Q_T), \quad u_n(0) = u_0 \text{ in } L^2(\Omega) \tag{39}$$

$$\int_{Q_T} \langle \partial_t u_n, \phi\rangle \, dt + \int_{Q_T} g(|\nabla(u_n)_\sigma|)|\nabla u_n|^{p(x)-2}\nabla u_n \nabla\phi \, dxdt = \int_{Q_T} f_n(t,x,u_n)\phi \, dxdt \tag{40}$$

for all test function $\phi \in \mathcal{V}$. The starting point is to show that the approximate solution u_n is nonnegative. The main idea is based on the construction of a special test function and the use of the assumptions $(\mathcal{H}_2)$ and $(\mathcal{H}_3)$.

Lemma 2. Let (u_n) be the sequence defined as above. Then, we have

$$u_n(t,x) \ge 0 \text{ a.e in } Q_T. \tag{41}$$

Proof. Let $\epsilon > 0$, we consider the function $\tau_\epsilon(s)$ defined as follows

$$\tau_\epsilon(s) = \begin{cases} -\frac{1}{\epsilon} + \frac{1}{\epsilon}\exp\left(-\epsilon s - \epsilon^2 \ln(|\frac{s-\epsilon}{\epsilon}|)\right) & \text{if } s < 0 \\ 0 & \text{if } s \ge 0. \end{cases}$$

It is easy to verify that $\tau_\epsilon(s)$ is a sequence of convex functions such as

- $\tau_\epsilon'(s)$ is bounded for all $s \in \mathbb{R}$
- $\tau_\epsilon'(s) \to sign^-(s)$ when $\epsilon \to 0$
- $\tau_\epsilon(s) \to (s)^-$ when $\epsilon \to 0$

where $sign^-$ is the following sign function

$$sign^-(r) = \begin{cases} -1 & \text{if } r < 0 \\ 0 & \text{if } r \geq 0. \end{cases}$$

By taking $\phi = \tau_\epsilon'(u_n)\chi_{(0,t)}$ as a test function in (40), one obtains

$$\int_\Omega \big(\tau_\epsilon(u_n)(t) - \tau_\epsilon(u_n)(0)\big)\,dx + \int_{Q_t} g(|\nabla(u_n)_\sigma|)|\nabla u_n|^{p(x)}\tau_\epsilon''(u_n)\,dxdt = \int_{Q_t} f_n(t,x,u_n)\tau_\epsilon'(u_n)\,dxdt. \tag{42}$$

The fact the u_0 is nonnegative implies that

$$\int_\Omega \tau_\epsilon(u_n)(0)\,dx = \int_\Omega \tau_\epsilon(u_0)\,dx = 0.$$

Applying the convexity of the function $\tau_\epsilon(\cdot)$ and estimate (16), the equations (42) becomes

$$\int_\Omega \tau_\epsilon(u_n)(t)\,dx \leq \int_{Q_t} f_n(t,x,u_n)\tau_\epsilon'(u_n)\,dxdt \leq \int_{Q_t\cap\{u_n<0\}} f_n(t,x,u_n)\tau_\epsilon'(u_n)\,dxdt + \int_{Q_t\cap\{u_n\geq 0\}} f_n(t,x,u_n)\tau_\epsilon'(u_n)\,dxdt.$$

Let us remark that $\tau_\epsilon'(u_n) = 0$ on the set $\{u_n \geq 0\}$. We therefore have

$$\int_\Omega \tau_\epsilon(u_n)(t)\,dx \leq \int_{Q_t\cap\{u_n<0\}} f_n(t,x,u_n)\tau_\epsilon'(u_n)\,dxdt.$$

By letting $\epsilon \to 0$, one gets

$$\int_\Omega (u_n)^-(t)\,dx \leq -\int_{Q_t\cap\{u_n<0\}} f_n(t,x,u_n)\,dxdt.$$

In view of (8), we conclude that

$$\int_\Omega (u_n)^-(t) \leq 0,$$

by using the fact that $(u_n)^-(t) \geq 0$, we arrive at

$$u_n(t,x) \geq 0 \text{ a.e in } Q_T.$$

□

Remark 2. According to Lemma 2 and in view to the sign condition $(\mathcal{H}_3)$, one may deduce that

$$|f_n(t,x,u_n)| = -f_n(t,x,u_n). \tag{43}$$

This result makes the key to several passages in the proof of our main result.

4.2 | A priori estimates

The purpose of this section is to provide some a priori estimates on the approximate solution (u_n).

Lemma 3. Let (u_n) be the solution of the approximate problem (38). Then, we have

i)

$$\|u_n\|_{L^\infty(0,T;L^2(\Omega))} + 2\alpha \min\left\{\|u_n\|_{\mathcal{V}}^{p^-}, \|u_n\|_{\mathcal{V}}^{p^+}\right\} \leq \|u_0\|_{L^2(\Omega)}^2.$$

ii)

$$\int_{Q_T} \big|u_n f_n(t,x,u_n)\big|\,dxdt \leq \|u_0\|_{L^2(\Omega)}^2.$$

Proof. *i*) For $0 \le t \le T$, we take $\phi = u_n \chi_{(0,t)}$ as a test function in the weak formulation (40), one has

$$\frac{1}{2}\int_{\Omega} u_n^2(t)\,dx + \int_{Q_t} g(|\nabla(u_n)_\sigma|)|\nabla u_n|^{p(x)}\,dxdt = \frac{1}{2}\int_{\Omega} u_0^2\,dx + \int_{Q_t} u_n f_n(t,x,u_n)\,dxdt. \tag{44}$$

According to (8) and by using the relations (12) and (16), it follows that

$$\frac{1}{2}\int_{\Omega} u_n^2(t)\,dx + \alpha \min\left\{ \|u_n\|_{\mathcal{V}}^{p^-}, \|u_n\|_{\mathcal{V}}^{p^+} \right\} \le \frac{1}{2}\int_{\Omega} u_0^2\,dx.$$

Which implies that,

$$\|u_n\|_{L^\infty(0,T;L^2(\Omega))} + 2\alpha \min\left\{ \|u_n\|_{\mathcal{V}}^{p^-}, \|u_n\|_{\mathcal{V}}^{p^+} \right\} \le \|u_0\|_{L^2(\Omega)}^2.$$

ii) From the equations (44) it follows that

$$-\int_{Q_T} u_n f_n(t,x,u_n)\,dxdt \le \frac{1}{2}\int_{\Omega} u_0^2\,dx. \tag{45}$$

By employing the results of (41) and (43) in (45), we arrive at

$$\int_{Q_T} \left| u_n f_n(t,x,u_n) \right|\,dxdt \le \|u_0\|_{L^2(\Omega)}^2.$$

□

Lemma 4. Let (u_n) be the sequence defined as above. Then,

i) there exist a constant C such that

$$\int_{Q_T} \left| f_n(t,x,u_n) \right|\,dxdt \le C.$$

ii) the sequence $\left(g(|\nabla(u_n)_\sigma|)|\nabla u_n|^{p(x)-2}\nabla u_n \right)$ is bounded in $L^{p'(x)}(Q_T)$.

Proof. *i*) With the help of (9), one has

$$\begin{aligned}\int_{Q_T} \left| f_n(t,x,u_n) \right|\,dxdt &= \int_{Q_T\cap\{u_n\le 1\}} \left| f_n(t,x,u_n) \right|\,dxdt + \int_{Q_T\cap\{u_n>1\}} \left| f_n(t,x,u_n) \right|\,dxdt \\ &\le \int_{Q_T} h_1(t,x)\,dxdt + \int_{Q_T\cap\{u_n>1\}} \left| f_n(t,x,u_n) \right|\,dxdt.\end{aligned} \tag{46}$$

For the second integral, we have the following inequality

$$\int_{Q_T\cap\{u_n>1\}} \left| f_n(t,x,u_n) \right|\,dxdt \le -\int_{Q_T} u_n f_n(t,x,u_n)\,dxdt \le \int_{Q_T} \left| u_n f_n(t,x,u_n) \right|\,dxdt.$$

Using the result of *ii*) from Lemma 3, we get

$$\int_{Q_T\cap\{u_n>1\}} \left| f_n(t,x,u_n) \right|\,dxdt \le \|u_0\|_{L^2(\Omega)}^2. \tag{47}$$

In view to estimates (46) and (47), we deduce that $\left(f_n(t,x,u_n) \right)$ is bounded in $L^1(Q_T)$.

ii) For simplicity reasons, we will denoted by $\theta_n = g(|\nabla(u_n)_\sigma|)|\nabla u_n|^{p(x)-2}\nabla u_n$. To prove that (θ_n) is bounded in $L^{p'(x)}(Q_T)$, one may use (4). We get

$$\|\theta_n\|_{L^{p'(x)}(Q_T)} \le \max\left\{ \rho_{p'(x)}^{\frac{1}{(p')^-}}(\theta_n), \rho_{p'(x)}^{\frac{1}{(p')^+}}(\theta_n) \right\}. \tag{48}$$

By a direct computation, we have

$$\rho_{p'(x)}(\theta_n) = \int\limits_{Q_T} \left|\theta_n\right|^{p'(x)}\, dxdt = \int\limits_{Q_T} \left|g(|\nabla(u_n)_\sigma|)|\nabla u_n|^{p(x)-2}\nabla u_n\right|^{\frac{p(x)}{p(x)-1}}\, dxdt.$$

Thanks to the result of (32), we obtain

$$\rho_{p'(x)}(\theta_n) \leq C(\beta, p^-, p^+) \int\limits_{Q_T} |\nabla u_n|^{p(x)}\, dxdt \leq C(\beta, p^-, p^+) \max\left\{ \|u_n\|_{\mathcal{V}}^{p^-}, \|u_n\|_{\mathcal{V}}^{p^+} \right\}. \tag{49}$$

From the estimate ii) of Lemma 3, (49) and (48), we conclude that

$$\|\theta_n\|_{L^{p'(x)}(Q_T)} \leq C$$

where C is a constant depending only on $\alpha, \beta, p^-, p^+, \Omega$, and $\|u_0\|_{L^2(\Omega)}$. □

4.3 | Convergences and passing to the limit

In this section, we will establish necessary convergence results in order to pass to the limit on the approximate problem (38). According to Lemma 3, we know that (u_n) is bounded in $\mathcal{V}$ and by Lemma 4, we conclude that $\left(f_n(t,x,u_n)\right)$ is bounded $L^1(Q_T)$. Reasoning by the same manner as of Section 3, we can easily prove that $\left(\partial_t u_n\right)$ is bounded in $\mathcal{V}^* + L^1(Q_T)$. Then, by applying the compactness results of the Lemma 5.2 from [15], we deduce the existence of a subsequence denoted again by (u_n) for simplicity reasons such that

$$\begin{aligned} \left(u_n\right) &\to u \text{ strongly in } L^{p^-}(Q_T) \text{ and a.e. in } Q_T \\ \left(\nabla u_n\right) &\to \nabla u \text{ a.e. in } Q_T. \end{aligned}$$

Therefore, it result from ii) of the Lemma 4 that

$$\left(|\nabla u_n|^{p(x)-2}\nabla u_n\right) \rightharpoonup |\nabla u|^{p(x)-2}\nabla u \text{ weakly in } L^{p'(x)}(Q_T).$$

Let us sum up the previously obtained convergences, we have

$$\left(u_n\right) \rightharpoonup u \text{ weakly in } \mathcal{V} \tag{50}$$

$$\left(u_n\right) \to u \text{ strongly in } L^{p^-}(Q_T) \text{ and a.e. in } Q_T \tag{51}$$

$$\left(\nabla G_\sigma * u_n\right) \to \nabla G_\sigma * u \text{ strongly in } L^{p^-}(Q_T) \text{ and a.e. in } Q_T \tag{52}$$

$$\left(g\left(|\nabla G_\sigma * u_n|\right)\right) \to g\left(|\nabla G_\sigma * u|\right) \text{ strongly in } L^{p^-}(Q_T) \text{ and a.e. in } Q_T \tag{53}$$

$$\left(|\nabla u_n|^{p(x)-2}\nabla u_n\right) \rightharpoonup |\nabla u|^{p(x)-2}\nabla u \text{ weakly in } L^{p'(x)}(Q_T) \tag{54}$$

$$\left(f_n(t,x,u_n)\right) \to f(t,x,u) \text{ a.e. in } Q_T. \tag{55}$$

It remains to show that

$$\left(f_n(t,x,u_n)\right) \to f(t,x,u) \text{ strongly in } L^1(Q_T).$$

To prove this, we need to prove the following lemma.

Lemma 5. Let u_n be the solution of the approximate problem (38). Then, we have

$$\lim_{k\to+\infty} \sup_{n>0} \int\limits_{Q_T\cap\{u_n>k\}} \left|f_n(t,x,u_n)\right|\, dxdt = 0. \tag{56}$$

Proof. Let us remark that

$$k \int\limits_{Q_T\cap\{u_n>k\}} \left|f_n(t,x,u_n)\right|\, dxdt \leq -\int\limits_{Q_T\cap\{u_n>k\}} u_n f_n(t,x,u_n)\, dxdt \leq \int\limits_{Q_T} \left|u_n f_n(t,x,u_n)\right|\, dxdt.$$

Then, it results from ii) of Lemma 3 that

$$\int\limits_{Q_T\cap\{u_n>k\}} \left|f_n(t,x,u_n)\right|\, dxdt \leq \frac{\|u_0\|_{L^2(\Omega)}^2}{k},$$

which implies that

$$\lim_{k\to+\infty}\sup_{n>0}\int\limits_{Q_T\cap\{u_n>k\}}\left|f_n(t,x,u_n)\right|\,dxdt=0.$$

□

As a result, we have the following convergences.

Lemma 6. Let u_n be the sequence defined as above. Then, we have

$$\left(f_n(t,x,u_n)\right)\to f(t,x,u)\text{ strongly in }L^1(Q_T). \tag{57}$$

Proof. To prove that $(f_n(t,x,u_n))$ converges strongly in $L^1(Q_T)$, we propose to use the result of Vitali's lemma. According to the almost convergence (55), we know that we need only to prove that $(f_n(t,x,u_n))$ is equi-integrable in $L^1(Q_T)$ namely:

$$\forall\varepsilon>0,\exists\delta>0,\forall E\subset Q_T,\text{ if }|E|<\delta\text{ then }\int\limits_E|f_n(t,x,u_n)|\,dxdt\le\varepsilon.$$

Let E be a mesurable subset of Q_T, $\varepsilon>0$ and $k>0$, by a simple computation, we write

$$\int\limits_E|f_n(t,x,u_n)|\,dxdt=I_1(k)+I_2(k), \tag{58}$$

where

$$I_1(k)=\int\limits_{E\cap\{u_n>k\}}|f_n(t,x,u_n)|\,dxdt,\quad I_2(k)=\int\limits_{E\cap\{u_n\le k\}}|f_n(t,x,u_n)|\,dxdt.$$

For the first integral, we have the following inequality

$$I_1(k)\le\int\limits_{Q_T\cap\{u_n>k\}}|f_n(t,x,u_n)|\,dxdt.$$

By applying the result of (56), we deduce the existence of $k^*>0$, such that, for all $k\ge k^*$, we have

$$I_1(k)\le\frac{\varepsilon}{2}. \tag{59}$$

To deal with the second integral $I_2(k)$, we use the assumption (9), we obtain for all $k\ge k^*$,

$$I_2(k)\le\int\limits_E h_k(t,x)\,dxdt. \tag{60}$$

The fact that $h_k\in L^1(Q_T)$ implies that h_k is equi-integrable in $L^1(Q_T)$. Hence, there exists $\delta>0$ such that if $|E|\le\delta$, we have

$$\int\limits_E h_k(t,x)\,dxdt\le\frac{\varepsilon}{2}. \tag{61}$$

Finally, by using (58), (59) and (61), we deduce that $(f_n(t,x,u_n))$ is equi-integrable in $L^1(Q_T)$, which proves that $(f_n(t,x,u_n))$ converges strongly to $f(t,x,u)$ in $L^1(Q_T)$. □

5 | NUMERICAL DISCRETIZATION

We begin this paragraph by giving the appropriate choice of functions $g(\cdot)$, $p(\cdot)$ and the nonlinear term $f(u)$. In order to reduce the scattering in the high gradient areas, to preserve the contours and to keep it in the low gradient areas, we take

$$g(r,\lambda)=\frac{1}{1+\left(\frac{r}{\lambda}\right)^2}.$$

As mentioned before, we will use the choice of Black et al.[10] to define our noise estimator λ. Thus, we have

$$\lambda=\frac{1.4826}{\sqrt{2}}MAD(\nabla u), \tag{62}$$

where MAD denotes the median absolute deviation and can be computed as

$$MAD(\nabla u) = \text{median}\left[|\nabla u - \text{median}((|\nabla u|)|\right],$$

where median$(|\nabla u|)$ represents the median over the image u to the gradient amplitude. Concerning the choice of the exponent $p(\cdot)$, we take

$$p(x) = 1 + \frac{1}{1 + k\left|\nabla G_\sigma * u_0(x)\right|^2}, \tag{63}$$

where k and σ are nonnegative constants to be adjusted and u_0 is the initial blured image. The function $f(u)$ which expresses the nonlinearity in our model (1), is commonly chosen cubic (see Nagumo et al[47] and FitzHugh[26]), that is

$$f(u) = -\beta u(u-\alpha)(u-1).$$

The coefficient β adjusts the weight of the nonlinearity, where the second coefficient α is already known by the threshold of the nonlinearity. In the paper[46], Morfu et al. ensure the symmetry of the nonlinearity $f(u)$ by choosing $\alpha = \frac{1}{2}$. However, in our numerical expirement, we will take suitable values of coefficient (α, β) in order to compare our model to some known models in the literature.

There are numerous approaches to solve partial differential equations of this alike. The references[8,3,30,31,33,44], for example, provide various techniques. And since we are dealing with pixels in image processing, finite differences approaches and explicit schemes are the best options. We will feature a discretization of the suggested model defined by Equation (1) in the subsequent lines. Let us assume that τ is the time step size, we take

$$t = n\tau, \quad n = 0, 1, 2, \ldots$$
$$\begin{cases} x = i & 0 \le i \le M \\ y = j & 0 \le j \le N, \end{cases}$$

here (x, y) designates image pixel and $M \times N$ is the original image size. Let's denote by $u^n_{i,j}$ the approximation of $u(n\tau, i, j)$. We define the following discrete approximation

$$\nabla^+_x u^n_{i,j} = u^n_{i+1,j} - u^n_{i,j}, \quad \nabla^-_x u^n_{i,j} = u^n_{i,j} - u^n_{i-1,j}$$
$$\nabla^+_y u^n_{i,j} = u^n_{i,j+1} - u^n_{i,j}, \quad \nabla^-_y u^n_{i,j} = u^n_{i,j} - u^n_{i,j-1}.$$

Let us remark that the Gaussian kernel G_σ appears in two convolution terms which are that of $p(\cdot)$ and $g(\cdot)$. Hence, to avoid the use of a uniform value of G_σ, we propose to use two different parameters which are σ_1 and σ_2. According to the expression (63), we discretize $p(\cdot)$ as follows

$$p_{i,j} = 1 + \frac{1}{1 + k\left|\nabla G_{\sigma_1} * u_0\right|^2_{i,j}},$$

and we have

$$\lambda_n = \lambda(u^n), \quad g^n_{i,j} = g\left(\left|\nabla G_{\sigma_2} * u^n_{i,j}\right|, \lambda_n\right).$$

The discrete approximation of the divergence operator is expressed as:

$$\text{div}\left(g^n_{i,j}\,|\nabla u^n|^{p_{i,j}-2}\,\nabla u^n\right) = \nabla^-_x\left(g^n_{i,j}\,|\nabla u^n|^{p_{i,j}-2}\,\nabla^+_x u^n_{i,j}\right) + \nabla^-_y\left(g^n_{i,j}\,|\nabla u^n|^{p_{i,j}-2}\,\nabla^+_y u^n_{i,j}\right).$$

Then, the discrete explicit scheme of our proposed model (1) can be written as follows

$$u^{n+1}_{i,j} = u^n_{i,j} + \tau\,\text{div}\left(g^n_{i,j}\,|\nabla u^n|^{p_{i,j}-2}\,\nabla u^n\right) + \tau f\left(u^n_{i,j}\right), \tag{64}$$

where

$$u^0_{i,j} = u_0(ih, jh), \quad 0 \le i \le M,\ 0 \le j \le N.$$
$$u^n_{i,0} = u^n_{i,1}, \quad u^n_{0,j} = u^n_{1,j}, \quad u^n_{M,i} = u^n_{M-1,i}, \quad u^n_{i,N} = u^n_{i,N-1}.$$

Finally, we recall that the convolution of an image Y with the Gaussian kernel G_σ is defined by the following formula

$$\left(G_\sigma * u\right)(i,j) = \sum_{k_1=-1}^{k_1=1}\sum_{k_2=-1}^{k_2=1} G_\sigma\left(k_1, k_2\right) u\left(i - k_1, j - k_2\right).$$

6 | NUMERICAL EXPERIMENTS

We are aiming now to examine the validity of our theoretical results presented in the above sections for image enhancement and denoising. We will perform some numerical experiments on different types of images such as grayscale and color images. We shall compare the results of our model with some recent existing models which have shown their robustness not only in image enhancement but also in image denoising. To do so, we propose to compare our model with that of Alaa et al[2] and Guo et al[30]. In Figure 1 , we present the selected images for our numerical tests. In all the following numerical examples, we set the parameters of the nonlinearity f to $\beta = 1$ and $\alpha = 0.5$. At each iteration, we will calculate the parameter λ via the formula (62). We fix the processing times by choosing $T = 5$, $\tau = 0.01$ and we take $\sigma_1 = 0.7$, $\sigma_2 = 0.7$ and $k = 120$. We degrade each pixel of used images by a Gaussian noise for different values of noise estimator λ defined by equation (62).

Our choice of one image enhancement technique over another is based on the criterion called the EME enhancement measure or measure of improvement introduced in the paper[1] by Agaian et al. We will use this criterion to compare the quality of image enhancement. It is computed as follows: we divide the image u of size $M \times N$ into $k_1 \times k_2$ blocks $w_{k,l}(i,j)$ of sizes $l_1 \times l_2$, we put:

$$EME = \frac{1}{k_1 \times k_2} \sum_{l=1}^{k_2} \sum_{k=1}^{k_1} 20 \log \left(\frac{u^w_{\max;k,l}}{u^w_{\min;k,l}} \right),$$

where $u^w_{\min;k,l}$ and $u^w_{\max;k,l}$ are respectively minimum and maximum values of the image u inside the block $w_{k,l}$. To explain the behavior of the EME, we mention that when the EME increases indicate that the corresponding image is enhanced very well and vice versa. We shall use another criterion called $PSNR$ (Peak Signal-Noise Ratio) to measure the denoising robustness of our model. To define the expression of this criterion, we first introduce the so-called SNR (Signal-Noise Ratio) as follows

$$SNR = \frac{1}{M \times N} \sum_{i=1}^{M} \sum_{j=1}^{N} \left[u(i,j) - u_{ref}(i,j) \right]^2.$$

Therefore, the $PSNR$ is defined as

$$PSNR = 10 \log_{10} \left(\frac{255^2}{SNR} \right),$$

where u is the filtered image with one of the three models and u_{ref} is the reference image which is the one enhanced respectively without noise with one of the three models. The evaluation of the obtained $PSNR$ values behaves is like that of the EME, which means that a higher $PSNR$ value generally indicates that the reconstructed image is of higher quality. Thanks to the above criteria, we will use a stopping criterion to stop the iteration process of our algorithm. In our computation, we shall stop the global iteration process when the EME and $PSNR$ values become invariant, which means that the reconstructed image will have a better enhancement and denoising. We shall use another stopping criterion which will be based on the noise estimator λ. We choose to stop our algorithm when

$$\left| \lambda^{n+1} - \lambda^n \right| \leq 10^{-6},$$

which means that the algorithm iterations are repeated until that the relative variation in the noise estimator λ comes to be smaller than 10^{-6}.

Figures 2 , 3 , 4 and 5 present the numerical results of comparison between our approach and the algorithms of Alaa et al.[2] and that of Guo et al.[30] for used grayscale images. In Figures 6 , 7 , 8 and 9 , we compare the obtained numerical results for our model and the models of Alaa et al.[2] and Guo et al.[30] for used color images.

To explain the behaviors of the obtained images (Figure 2 -9), we list in Tables 1 and 2 a comparison of the reached EME and $PSNR$ values among the proposed model, Alaa et al.[2] and Guo et al.[30] for the used images. More precisely, Table 1 gives the EME and $PSNR$ values for the original image restored by our model and that of Alaa et al.[2] and Guo et al.[30]. Furthermore, Table 2 shows a comparison of EME and $PSNR$ values between our model, Alaa et al.[2] and Guo et al.[30] for selected images with respect to noise levels.

The analysis of the obtained images (see Figure 2 -9) confirms our hypothesis of the impact of noise on the three methods. Indeed, if we increase the noise estimator (λ), the images become noisier and the obtained numerical results show that our algorithm is more efficient (see Table 2) than those obtained by the two other algorithms. By comparing only the obtained $PSNR$ value listed in Table 2 , we can notice that our model is comparable to that of Guo et al.[30]. But taking into account the reached EME value, we can agree closely that our model leads to obtaining satisfactory results about image enhancement. This proves that our method is more robust to the nature of the noise. As it demonstrates the numerical simulations, the proposed model is, therefore, more efficient because it operates both on the filtering of the noise and on the improvement of the contrast.

FIGURE 1 Used images for numerical experiments: (1) eight; (2) lena; (3) football; (4) peppers.

TABLE 1 EME and PSNR comparison between the three methods Alaa et al[2], Guo at al[30] and proposed method for original images

Image	Alaa et al[2]		Guo et al[30]		Proposed	
	EME	PSNR	EME	PSNR	EME	PSNR
eight	5.78	66.36	2.20	84.77	**11.61**	**88.94**
lena	5.81	83.13	5.02	83.52	**10.21**	**102.03**
football	3.70	75.04	3.22	78.91	**11.29**	**88.98**
Peppers	7.02	76.38	6.87	84.33	**12.35**	**95.88**

TABLE 2 EME and PSNR comparison between the three methods Alaa et al[2], Guo at al[30] and proposed method for used images with respect to noise levels

Image	Noise estimator	Alaa et al[2]		Guo et al[30]		Proposed	
		EME	PSNR	EME	PSNR	EME	PSNR
eight	$\lambda = 0.115$	3.65	67.87	1.81	77.41	**10.45**	**79.54**
	$\lambda = 0.359$	3.26	66.59	1.57	76.98	**9.75**	**78.81**
lena	$\lambda = 0.113$	4.83	78.59	3.51	81.84	**9.92**	**83.13**
	$\lambda = 0.141$	4.31	76.44	3.39	81.28	**9.35**	**81.91**
football	$\lambda = 0.125$	3.43	74.65	3.17	78.33	**9.65**	**79.16**
	$\lambda = 0.151$	3.29	74.52	3.03	77.99	**9.13**	**78.47**
peppers	$\lambda = 0.107$	6.45	76.04	6.13	82.46	**11.56**	**83.11**
	$\lambda = 0.133$	6.11	75.87	6.01	81.58	**10.71**	**82.34**

Furthermore, by comparing the restored images, we can notice that our algorithm preserves the contours details of the images, while the other two models eliminate certain details of the images which explains the appearance of a weak blur.

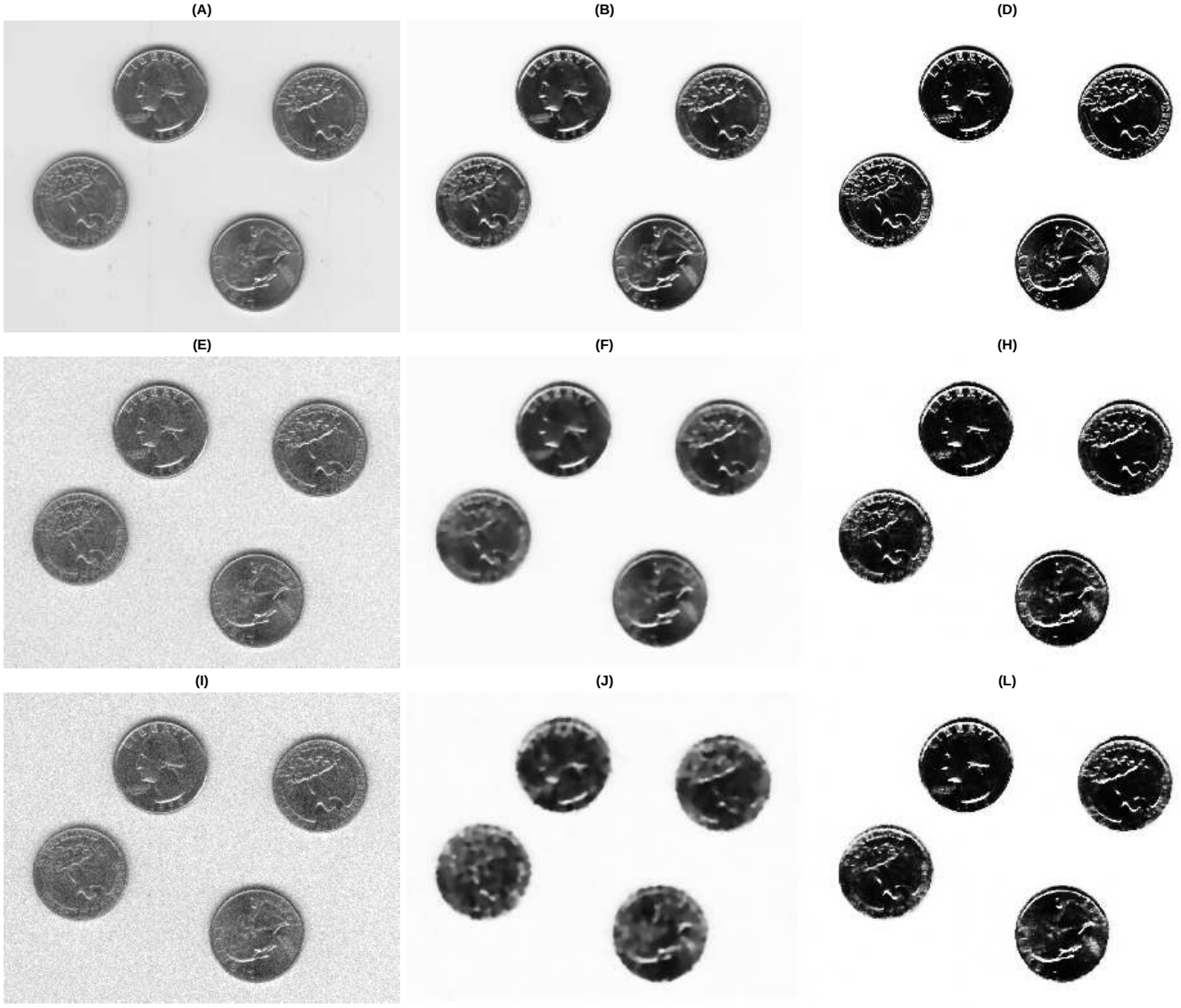

FIGURE 2 (A) Original image; (B) Original image restored by Alaa et al[2]; (D) Original image restored by the proposed method; (E) and (I) Noisy images for different noise levels; (F) and (J) Noisy images restored Alaa et al[2]; (H) and (L) Noisy images restored by the proposed method.

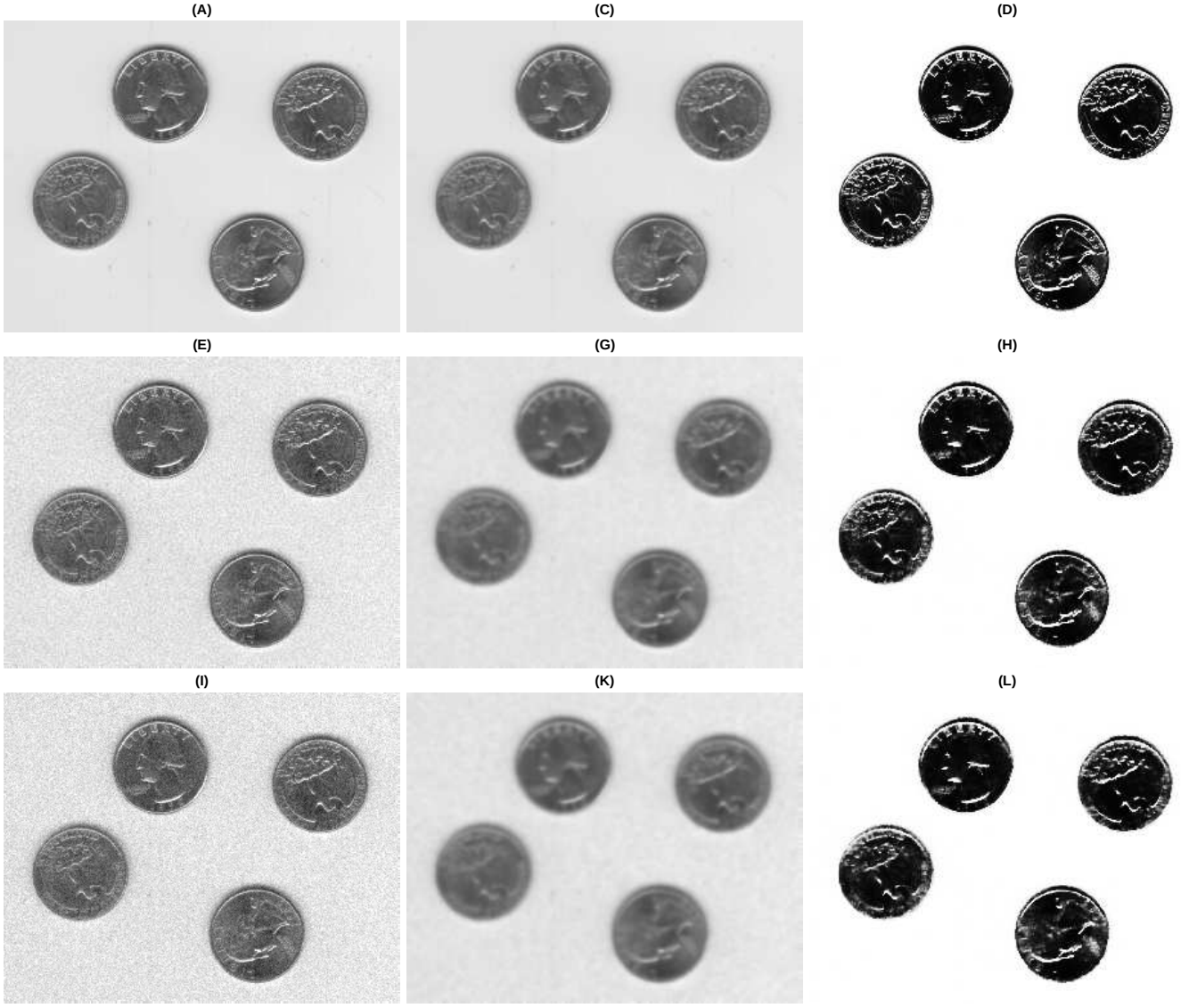

FIGURE 3 (A) Original image; (C) Original image restored by Guo et al[30]; (D) Original image restored by the proposed method; (E) and (I) Noisy images for different noise levels; (G) and (K) Noisy images restored Guo et al[30]; (H) and (L) Noisy images restored by the proposed method.

FIGURE 4 (A) Original image; (B) Original image restored by Alaa et al[2]; (D) Original image restored by the proposed method; (E) and (I) Noisy images for different noise levels; (F) and (J) Noisy images restored Alaa et al[2]; (H) and (L) Noisy images restored by the proposed method.

FIGURE 5 (A) Original image; (C) Original image restored by Guo et al[30]; (D) Original image restored by the proposed method; (E) and (I) Noisy images for different noise levels; (G) and (K) Noisy images restored Guo et al[30]; (H) and (L) Noisy images restored by the proposed method.

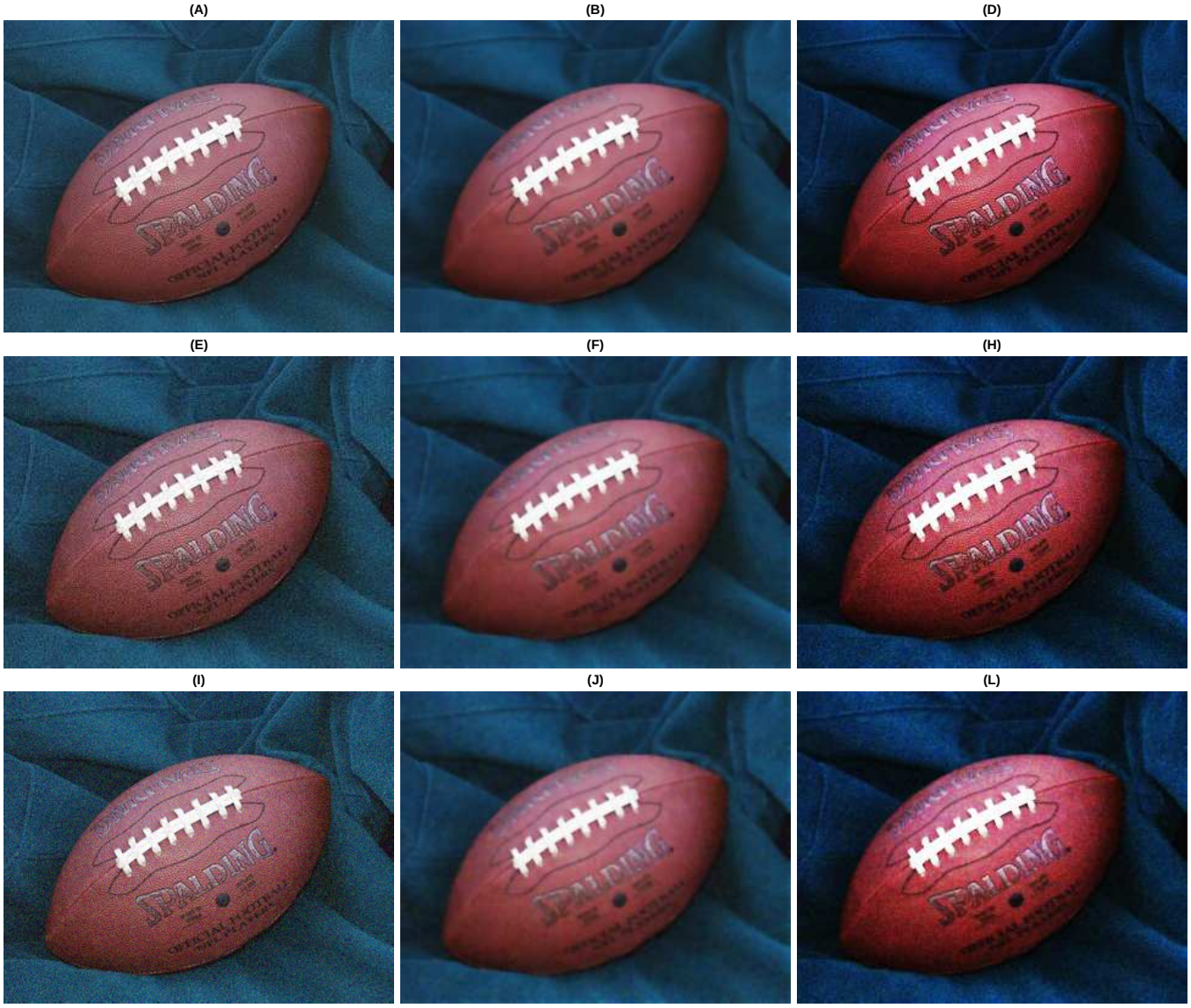

FIGURE 6 (A) Original image; (B) Original image restored by Alaa et al[2]; (D) Original image restored by the proposed method; (E) and (I) Noisy images for different noise levels; (F) and (J) Noisy images restored Alaa et al[2]; (H) and (L) Noisy images restored by the proposed method.

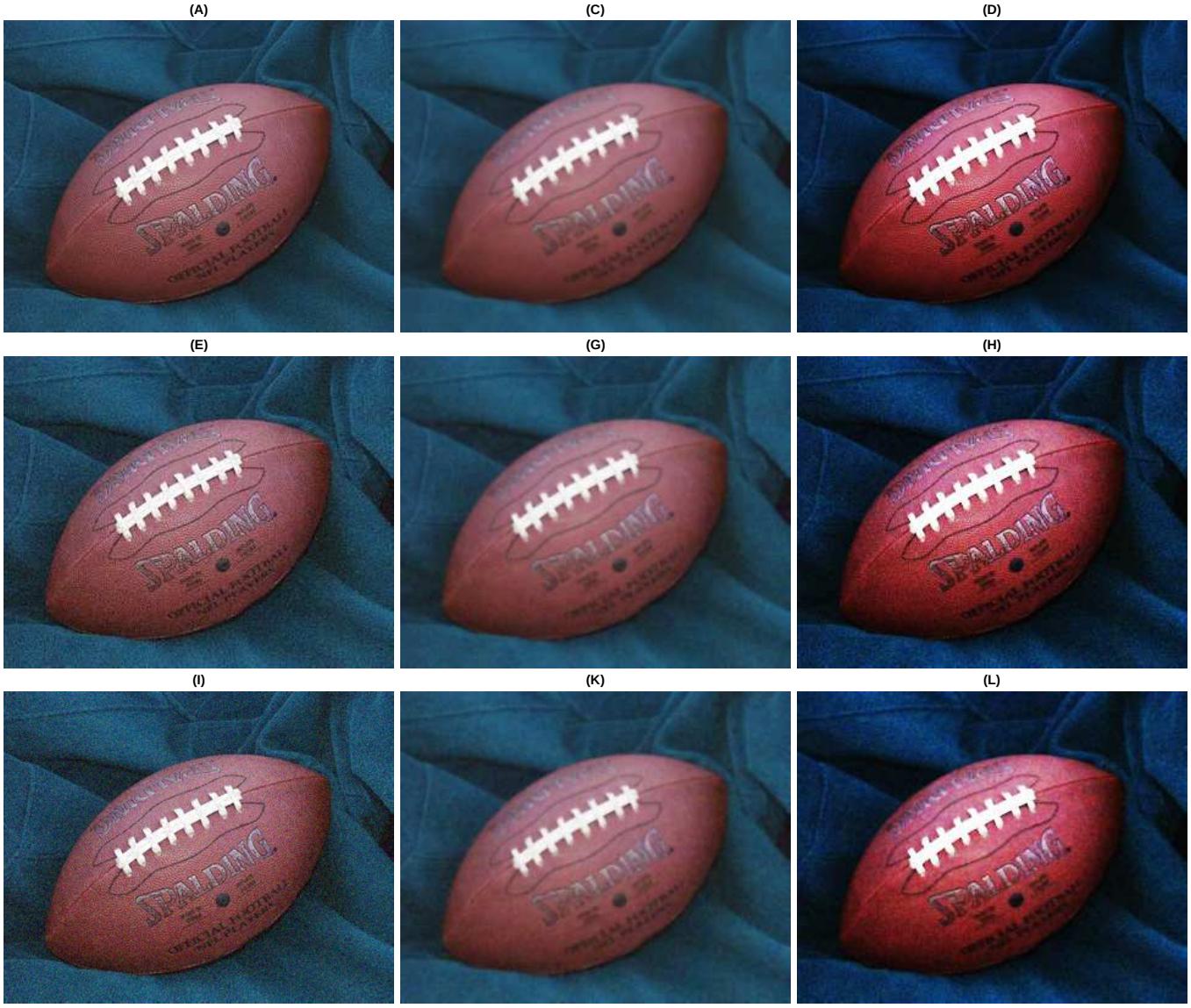

FIGURE 7 (A) Original image; (C) Original image restored by Guo et al[30]; (D) Original image restored by the proposed method; (E) and (I) Noisy images for different noise levels; (G) and (K) Noisy images restored Guo et al[30]; (H) and (L) Noisy images restored by the proposed method.

FIGURE 8 (A) Original image; (B) Original image restored by Alaa et al[2]; (D) Original image restored by the proposed method; (E) and (I) Noisy images for different noise levels; (F) and (J) Noisy images restored Alaa et al[2]; (H) and (L) Noisy images restored by the proposed method.

FIGURE 9 (A) Original image; (C) Original image restored by Guo et al[30]; (D) Original image restored by the proposed method; (E) and (I) Noisy images for different noise levels; (G) and (K) Noisy images restored Guo et al[30]; (H) and (L) Noisy images restored by the proposed method.

7 | CONCLUSION

We have proposed a novel nonlinear parabolic PDE with a nonstandard growth condition to enhance and restore a class of noisy images. Under the consideration of generalized Lebesgue and Sobolev spaces with variable exponent, we have proved two existence results of weak solutions to the proposed model. In the first, we have assumed that the nonlinearity is bounded by a suitable constant. Based on Schauder fixed point method, we have shown the existence of a weak solution to the considered problem. Secondly, we studied the proposed model in a general framework. We assumed only that the nonlinearity satisfies some weak hypotheses that involve a sign condition and without additional growth conditions. With the help of our first existence result and by using the truncations method, we have established the existence of a nonnegative weak solution to the proposed model. We have examined the efficiency of our model by realizing some numerical experiments with different image types. To highlight our challenge, we have compared our proposed model to some recent models which are known for their efficiency in image processing. Numerically the obtained images demonstrate that the proposed model gives reliable enhancement results for different types of images not only grayscale ones but also those with color. We have demonstrated numerically the robustness of our model by adding various levels of Gaussian type noise to the selected test images. By analyzing the obtained EME and $PSNR$ values, we have noticed that our method gives satisfactory results not only for image enhancement but also for denoising blurry images. To conclude, the proposed model shows great promise as a numerical tool for image enhancement/denoising, it could improve the resolution for different types of images.

ACKNOWLEDGEMENT

The authors would like to express their sincere gratitude to the anonymous referees and the handling editor for their careful reading of the manuscript.

References

1. S.S. Agaian, K. Panetta, A.M. Grigoryan, *A new measure of image enhancement*, In IASTED International Conference on Signal Processing and Communication, September, (2000), 19–22.
2. M. Ait Oussous, N. Alaa and Y. Ait Khouya, *Anisotropic and nonlinear diffusion applied to image enhancement and edge detection*, Int. J. Computer Applications in Technology, (2014) 122–133.
3. H. Alaa, N. E. Alaa and A. Charkaoui, *Time periodic solutions for strongly nonlinear parabolic systems with $p(x)$-growth conditions*. Journal of Elliptic and Parabolic Equations (2021) https://doi.org/10.1007/s41808-021-00118-9.
4. N. E. Alaa and M. Zirhem, *Bio-inspired reaction diffusion system applied to image restoration*, International Journal of Bio-Inspired Computation, **12**, 2 (2018), 128–137.
5. N. E. Alaa, M. Aitoussous, W. Bouarifi, D. Bensikaddour, *Image restoration using a reaction-diffusion process*. Electronic Journal of Differential Equations, 2014 (197), 1–12.
6. S. Antontsev, S. Shmarev, *Evolution PDEs with Nonstandard Growth Conditions: Existence, Uniqueness, Localization, Blow-up*, Atlantis Studies in Differential Equations, vol. **4**, Atlantis Press, Paris, 2015.
7. G. Arumugam, J. Tyagi, *Nonnegative solutions to reaction-diffusion system with cross-diffusion and nonstandard growth conditions*. Mathematical Methods in the Applied Sciences, **43**(10), (2020), 6576–6597.
8. G. Aubert, P. Kornprobst, *Mathematical problems in image processing: partial differential equations and the calculus of variations*, Vol **147**, New York: Springer (2006).
9. N. Beaudoin and S. Beauchemin. *An accurate discrete fourier transform for image processing*. In 2002 International Conference on Pattern Recognition, **3**, (2002), 935–939.
10. M.J. Black, G. Sapiro, D.H. Marimont, D. Heeger, *Robust anisotropic diffusion*, IEEE Trans. Image Processing, **7**, 3, (1998), 421–432.

11. L. Blanc-Feraud, P. Charbonnier, G. Aubert, and M. Barlaud. *Nonlinear image processing: modeling and fast algorithm for regularization with edge detection*. In Proceedings., International Conference on Image Processing, **1**, (1995), 474–477.

12. M. Bendahmane, P. Wittbold, A. Zimmermann, *Renormalized solutions for a nonlinear parabolic equation with variable exponents and L^1-data*, J. Differential Equations, **249**, 6 (2010), 1483–1515.

13. F. Catté, P-L. Lions, J-M. Morel, T. Coll, *Image selective smoothing and edge detection by nonlinear diffusion*, SIAM J. Numer. Anal, **29** 1, (1992), 182–193.

14. P. Charbonnier, L. Blanc-Feraud, G. Aubert, M. Barlaud, *Two deterministic half-quadratic regularization algorithms for computed imaging*, Proc. IEEE Int. Conf. Image. Processing, **2**, (1994), 168–172

15. A. Charkaoui, H. Fahim, N. E. Alaa, *Nonlinear parabolic equation having nonstandard growth condition with respect to the gradient and variable exponent*, Opuscula Math. **41**, no 1, (2021), 25–53.

16. A. Charkaoui, L. Taourirte, N. E. Alaa, *Periodic parabolic equation involving singular nonlinearity with variable exponent*. Ricerche mat (2021). https://doi.org/10.1007/s11587-021-00609-w.

17. A. Charkaoui and N. E. Alaa, *Existence and uniqueness of renormalized periodic solution to a nonlinear parabolic problem with variable exponent and L^1 data*. Journal of Mathematical Analysis and Applications (2022), 125674.

18. W. K. Chen, *The electrical engineering handbook*. Elsevier (2004).

19. Y. Chen, S. Levine, and M. Rao, *Variable exponent, linear growth functionals in image restoration*, SIAM journal on Applied Mathematics **66**, 4 (2006), 1383–1406.

20. J. M. B. Coll, A. Buades. *The staircasing effect in neighborhood filters and its solution*. IEEE transactions on image processing : a publication of the IEEE Signal Processing Society, **15**, (2006), 1499–505.

21. M. Demi, *New approach to automatic contour detection from image sequences: An application to ventriculographic images*. Computers and Biomedical Research, **27**(3), (1994), 157–177.

22. L. Diening, P. Harjulehto, P. Hästö and M. Ružička, *Lebesgue and Sobolev spaces with variable exponents*, volume 2017 of Lecture Notes in Mathematics. Springer, Heidelberg, 2011.

23. C. Fan and F. Zhang, *Homomorphic filtering based illumination normalization method for face recognition*. Pattern Recognition Letters, **32**(10), (2011) 1468–1479.

24. X. Fan, and D. Zhao, *On the spaces $L^{p(x)}(\Omega)$ and $W^{m,p(x)}(\Omega)$*. Journal of Mathematical Analysis and Applications, **263**, 2 (2001), 424–446.

25. L. Fan, F. Zhang, H.Fan, *Brief review of image denoising techniques*. Vis. Comput. Ind. Biomed. Art, (2019).

26. R. FitzHugh, *Impulses and physiological states in theoretical models of nerve membrane*, Biophysical Journal, **1**, No. 6, (1961), 445–466.

27. Z. H. Gebeyehu, *Impact of clipping noise on the sum rate of NOMA with PD-DCO-OFDM and conventional DCO-OFDM*. Heliyon, **6**(2), (2020), e03363.

28. G. Gilboa, Y. Zeevi, *Image enhancement, segmentation and denoising by time dependent nonlinear diffusion processes*, Proceedings of the International Conference on Image Processing, ICIP01, Thesalonik, Greece, **3**, (2001), 134–137.

29. A. González-Díez, J. A. Barreda-Argüeso, L. Rodríguez-Rodríguez, J. Fernández-Lozano, *The use of filters based on the Fast Fourier Transform applied to DEMs for the objective mapping of karstic features*. Geomorphology, **385**, (2021), 107724.

30. Z. Guo, Q. Liu, J. Sun, B. Wu, *Reaction-diffusion systems with $p(x)$-growth for image denoising*. Nonlinear Analysis: Real World Applications, **12**(5), 2904–2918, (2011).

31. F. Karami, L. Ziad, K. Sadik, *A splitting algorithm for a novel regularization of Perona-Malik and application to image restoration*. EURASIP Journal on Advances in Signal Processing, (2017), 1–9.

32. F. Karami, K. Sadik, L. Ziad, *A variable exponent nonlocal p (x)-Laplacian equation for image restoration*. Computers & Mathematics with Applications, **75**(2), (2018), 534–546.

33. F. Karami, D. Meskine, K. Sadik, *A new nonlocal model for the restoration of textured images*. Journal of Applied Analysis & Computation, **9**(6), (2019), 2070–2095.

34. J. Kim, J. Kim, S. Jung, C. Noh, S. Ko. *Novel contrast enhancement scheme for infrared image using detail-preserving stretching*. Optical Engineering, **50**(7), July 2011.

35. J.J. Koenderink, *The structure of images*, Biol. Cybern, **50**, (1984), 363–370.

36. E. Konukoglu, M. Sermesant, O. Clatz, J. Peyrat, H. Delingette, and N. Ayache. *A recursive anisotropic fast marching approach to reaction diffusion equation: Application to tumor growth modeling*. In N. Karssemeijer and B. Lelieveldt, editors, Information Processing in Medical Imaging, Berlin, Heidelberg, Springer Berlin Heidelberg, (2007), 687–699.

37. O. Kováčik, and J. Rákosník; *On spaces $L^{p(x)}$ and $W^{k,p(x)}$*, Czechoslovak mathematical journal, **41**, 4 (1991), 592–618.

38. M. Kumar and S. Dass, *A total variation-based algorithm for pixel-level image fusion*. IEEE Transactions on Image Processing, **18**(9), (2009), 2137–2143.

39. L. H. Lee, T. Braud, P. Zhou, L. Wang, D. Xu, Z. Lin, P. Hui, *All one needs to know about metaverse: A complete survey on technological singularity, virtual ecosystem, and research agenda*. (2021) arXiv preprint arXiv:2110.05352.

40. Z. Li, W. Gao, *Existence of renormalized solutions to a nonlinear parabolic equation in L^1 setting with nonstandard growth condition and gradient term*, Mathematical Methods in the Applied Sciences. **38** (14), (2015), 3043–3062.

41. X. Li, T. Chen, *Nonlinear diffusion with multiple edginess thresholds*, Pattern Recognition, **27** 8, (1994), 1029–1037.

42. J. L. Lions, *Quelques méthodes de résolution des problèmes aux limites non linéaires.* Paris: Dunod et GauthiersVillars, (1969).

43. X. Liu, D. Wang, *A spectral histogram model for texton modeling and texture discrimination*. Vision Research, **42**(23), (2002), 2617–2634.

44. W. Lu, J. Duan, Z. Qiu, Z. Pan, R. W. Liu, L. Bai, *Implementation of high-order variational models made easy for image processing*. Mathematical Methods in the Applied Sciences, **39**(14), (2016), 4208–4233.

45. H. Mitchell, N. Mashkit, *Noise smoothing by a fast k-nearest neighbour algorithm*. Signal Processing: Image Communication, **4**(3), (1992), 227–232.

46. S. Morfu, P. Marquie, B. Nofiele, D. Ginhac, *Nonlinear systems for image processing*, Advances in Imaging and Electron Physics, Elsevier, **152**, (2008), 79–153.

47. J. Nagumo, S. Arimoto, S. Yoshizawa, *An active pulse transmission line simulating nerve axon*, Proceedings of the I.R.E, **50**, No. 10, (1962), 2061–2070.

48. S. Osher, A. Sole, and L. Vese. *Image decomposition and restoration using total variation minimization and the $H^{-}1$ norm*. SIAM: Multiscale Model Sim, (2003).

49. N. Papageorgiou, V. Rădulescu, D. Repovš; *Nonlinear Analysis-Theory and Methods*, Springer Monographs in Mathematics, (2019).

50. P. Perona, J. Malik, *Scale space and edge detection using anisotropic diffusion*, IEEE Trans, Pattern Anal. Mach. Intell, **12**, 7, (1990), 629–639.

51. V. Rădulescu and D. Repovš; *Partial differential equations with variable exponents: variational methods and qualitative analysis*, Chapman and Hall/CRC (2015).

52. V. Rădulescu, *Isotropic and anisotropic double-phase problems: old and new*, Opuscula Math. **39**, (2019), 259–279.

53. Ruzicka, Michael; *Electrorheological fluids: modeling and mathematical theory*, Springer Science & Business Media, (2000).

54. L. Shangerganesh, K. Balachandran, *Solvability of reaction-diffusion model with variable exponents*, Math. Methods Appl. Sci. **37**, 10, (2014), 1436–1448.

55. J. Simon, *Compact sets in the space* $L^p(0,T;B)$, Ann. Mat. Pura Appl. **146**, 4 (1987), 65–96.

56. D. Strong and T. Chan. *Spatially and scale adaptive total variation based regularization and anisotropic diffusion*. Image Processing, (1996).

57. S. Tang, L. Xiao, *Image zooming based on residuals*. In T. Tan, Q. Ruan, X. Chen, H. Ma, and L. Wang, editors, Advances in Image and Graphics Technologies, pages 307–314, Berlin, Heidelberg, (2013). Springer Berlin Heidelberg.

58. S. Tebini, H. Seddik, and E. Braiek. *An advanced and adaptive mathematical function for an efficient anisotropic image filtering*. Computers & Mathematics with Applications, **72**(5), (2016), 1369–1385.

59. S. Villar, S. Torcida, and G. Acosta. *Median filtering: A new insight*. Journal of Mathematical Imaging and Vision, **58**, (2017),1–17

60. F. Voci, S. Eiho, N. Sugimoto, H. Sekiguchi, *Estimating the gradient threshold in the Perona-Malik equation*, IEEE Signal Process. Mag, **21** 3, (2004), 39–65.

61. C. Zhang, S. Zhou, *Renormalized and entropy solutions for nonlinear parabolic equations with variable exponents and* L^1 *data*, J. Differential Equations, **248**, 6 (2010), 1376–1400.

□